

Hindlimb perfusion was measured serially with laser Doppler imaging (Figure 1, A and B). SDF-1 α gene transfer increased blood flow recovery on days 7, 14, 21, and 28 after ischemia. The SDF-1 α -induced enhancement of blood perfusion was suppressed by blockade of VEGF by sFlt-1 gene transfer or by inhibition of NO synthesis by treatment with L-NAME. Combined treatment with sFlt-1 and L-NAME did not have further inhibitory effects.

Capillary density was determined by immunohistochemical staining with anti-CD31 antibody on day 28 (Figure 1C). SDF-1 α gene transfer to the nonischemic limb did not affect capillary density; however, it enhanced capillary density of the ischemic hindlimb compared with the level observed in the nonischemic hindlimb or ischemic hindlimb. No SDF-1 α -induced increase in capillary density was seen in the sFlt-1, L-NAME, or L-NAME+sFlt-1 groups.

Effects of SDF-1 α Gene Transfer on EPC Mobilization and Incorporation in BMT Mice

Mobilization of EPCs to the peripheral circulation was determined by flow cytometry 14 days after ischemia. SDF-1 α gene transfer to nonischemic normal mice did not significantly affect the percentage of CD31- and c-kit-positive EPCs (Figure 2, A and B). In contrast, SDF-1 α gene transfer to ischemic mice induced mobilization of EPCs (Figure 2, A and B). This SDF-1 α -induced EPC mobilization was blunted in the sFlt-1, L-NAME, and L-NAME+sFlt-1 groups (Figure 2A).

To assess incorporation of bone marrow lineage cells to neovascularization, the percentage of capillaries positive for both LacZ and CD31 to total CD31 staining capillaries was calculated on day 28 (Figure 2, C and D). SDF-1 α gene transfer to nonischemic normal mice did not affect the percentage of LacZ-positive capillaries. In contrast, SDF-1 α gene transfer to the ischemic hindlimb significantly increased incorporation of LacZ-positive cells into the capillary vessels, which was blunted in the sFlt-1, L-NAME, and L-NAME+sFlt-1 groups (Figure 2, C and D). There was only a partial incorporation of LacZ-positive cells into the microvessels (only 12% of capillaries were LacZ-positive), suggesting that SDF-1 α gene transfer enhanced not only ischemia-induced vasculogenesis but also angiogenesis.

Effects of SDF-1 α on EPC Mobilization and Incorporation Into Neovessels

Because incorporation of LacZ-positive cells into capillary vessels might not prove incorporation of EPCs, an *in vivo* matrigel plug assay was performed to determine the SDF-1 α -induced incorporation of EPC lineage cells into neovessels in both wild-type and BMT mice (Figure 3). Matrigels containing SDF-1 α protein had significant neovessel formation in wild-type and BMT^{LacZ} \rightarrow ^{wild} mice (Figure 3). Fluorescence microscopy revealed that most CD31-positive neovessels contained c-kit- and CXCR4-expressing cells, suggesting that CXCR4-positive EPCs might mobilize into the SDF-1 α -containing Matrigels, resulting in neovessel formation.

Regulation of VEGF, phospho-Akt, and phospho-eNOS Protein Levels in BMT Mice

VEGF protein content increased in the ischemic muscles compared with nonischemic controls at 14 days of treatment.

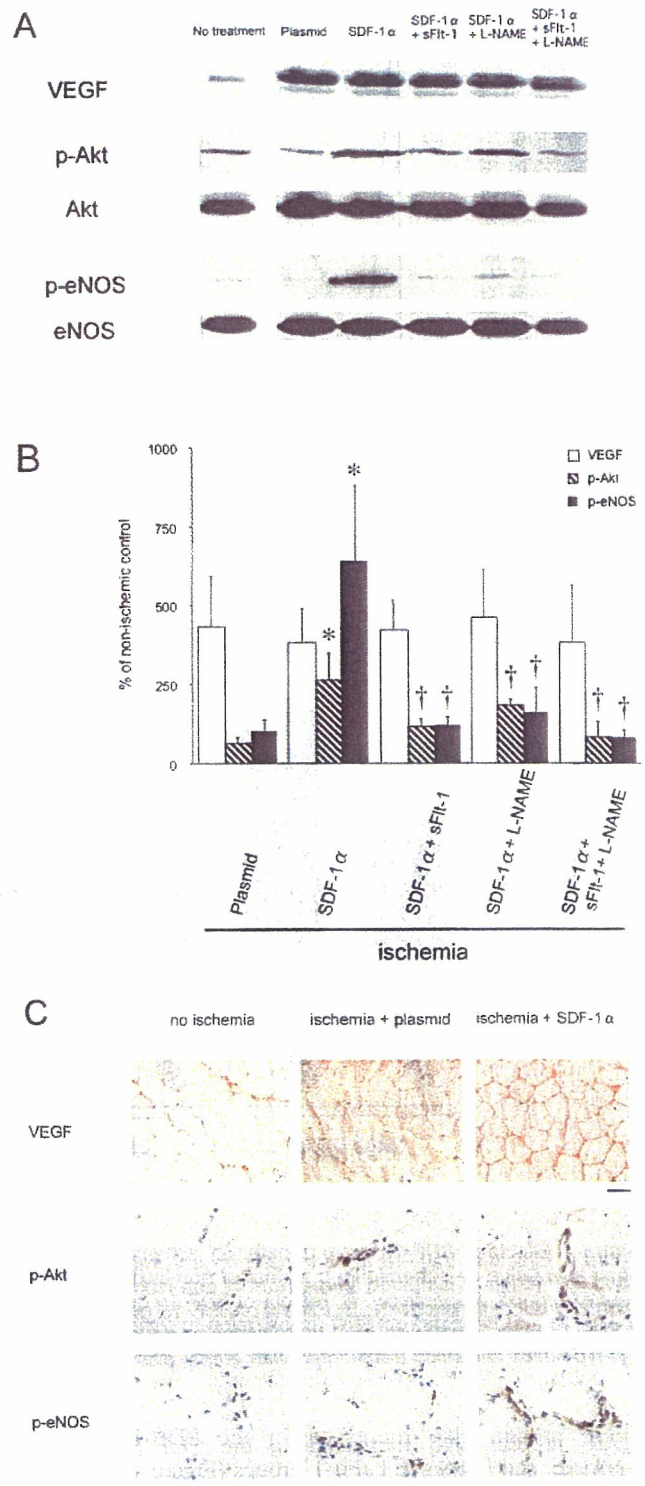


Figure 3. Regulation of VEGF, phospho-Akt, and phospho-eNOS protein in plasmid (n=5), SDF-1 α (n=5), SDF-1 α +sFlt-1 (n=5), SDF-1 α +L-NAME (n=5), and SDF-1 α +L-NAME+sFlt-1 (n=5) groups. A, Western blot of VEGF, phospho-Akt, and phospho-eNOS proteins in ischemic and non-ischemic muscle 7 days after ischemia. B, Quantitative evaluation of VEGF, phospho-Akt, and phospho-eNOS protein levels expressed as a percentage of non-ischemic control. * P <0.05 vs plasmid group; † P <0.05 vs ischemia+SDF-1 α . C, Pictures of ischemic muscle sections stained immunohistochemically with antibodies against VEGF, phospho-Akt, and phospho-eNOS protein. Scale bar: 50 μ m.

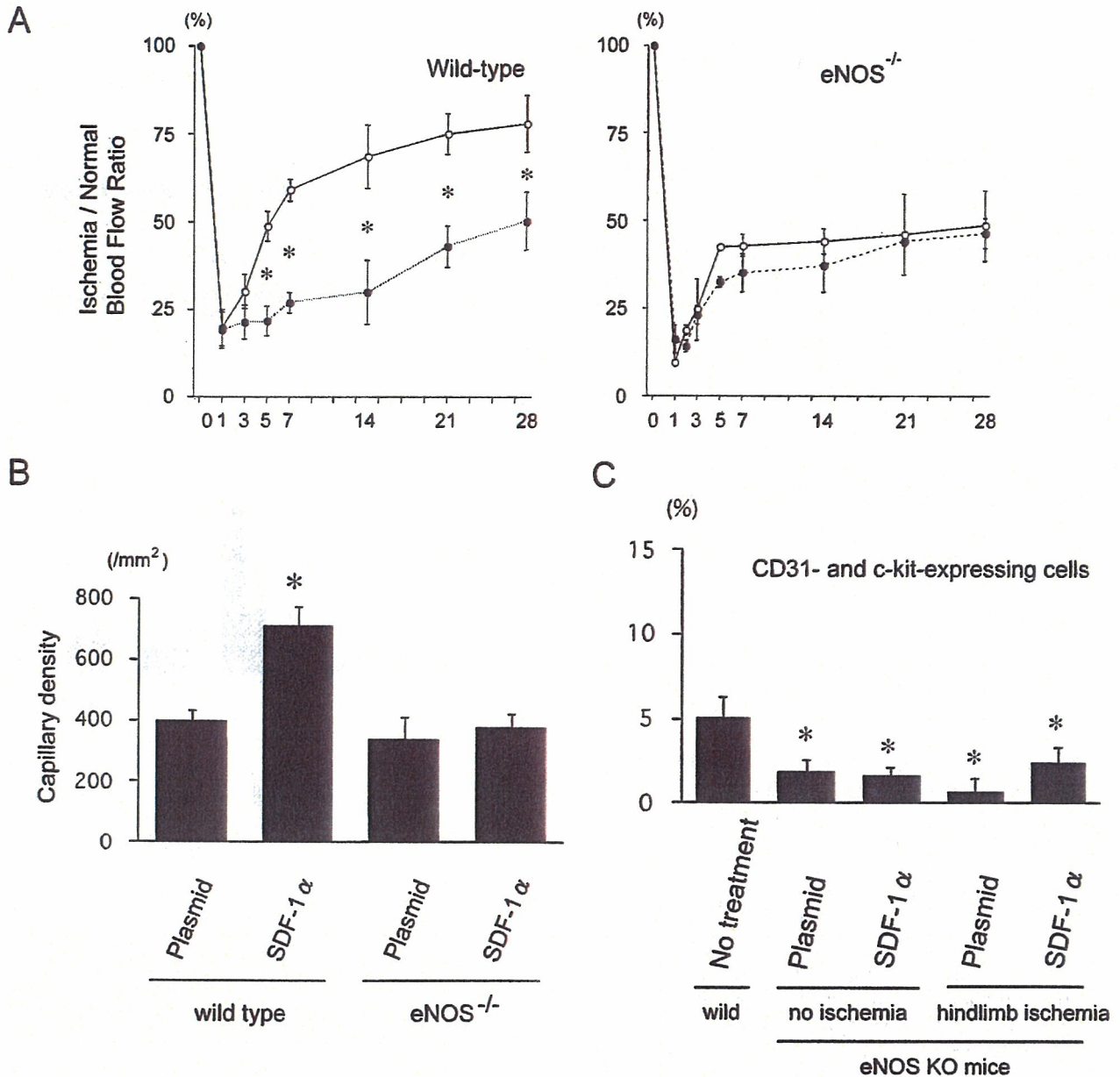


Figure 4. Effects of SDF-1 α gene transfer on ischemia-induced neovascularization in wild-type and eNOS^{-/-} mice. **A**, Summary of the blood flow ration of ischemic limb to that of non-ischemic limb. Open and closed circles indicate SDF-1 α gene transfer and empty plasmid groups, respectively. **B**, Effects of SDF-1 α gene transfer on capillary density. N=7 to 8. **P*<0.05 vs plasmid group. **C**, Effects of SDF-1 α gene transfer on EPC mobilization to peripheral circulation CD31 and c-kit double-positive cells is presented in non-treated wild type mice and mice transfected with empty plasmid or SDF-1 α gene into ischemic muscles. **P*<0.01 vs no treatment.

VEGF protein also increased in the SDF-1 α , sFlt-1, L-NAME, and L-NAME+sFlt-1 groups (Figure 4A). Immunohistochemistry revealed that increased VEGF was localized in ischemic myocytes (Figure 4B). In contrast, phospho-Akt and phospho-eNOS were localized in microvascular endothelial cells, and their intensity was enhanced by SDF-1 α transfection. Neither phospho-Akt nor phospho-eNOS protein levels changed in ischemic muscle of the plasmid group, but they were increased in SDF-1 α -transfected ischemic muscle. The SDF-1 α -induced increases in phospho-Akt and phospho-eNOS protein levels were blunted in the sFlt-1, L-NAME, and L-NAME+sFlt-1 groups (Figure 4B).

Effects of SDF-1 α Gene Transfer on Ischemia-Induced Neovascularization in eNOS^{-/-} Mice

SDF-1 α gene transfer augmented recovery of blood perfusion, increased capillary density, and EPC mobilization in wild-type (eNOS^{+/+}) mice as in BMT^{LacZ}→^{Wild} mice. In contrast, such SDF-1 α -induced effects were blunted in eNOS^{-/-}.

Discussion

The novel finding of this study is that intramuscular gene transfer of SDF-1 α (a strong EPC chemoattractant) into

ischemic limbs enhanced ischemia-induced neovascularization in mice associated with mobilization and partial incorporation of EPC into neovessels. Salcedo et al¹⁷ reported that serial intradermal injections of SDF-1 α protein into mouse skin induced significant microvessel formation associated with recruitment of leukocytes, which was equipotent to neovessel formation induced by VEGF protein injections. These previous studies, however, did not address whether SDF-1 α induces therapeutic angiogenesis, vasculogenesis, or both in vivo. Using BMT^{LacZ \rightarrow Wild} mice, we demonstrated that SDF-1 α gene transfer enhanced both ischemia-induced vasculogenesis and angiogenesis in vivo.

To investigate the mechanisms underlying the SDF-1 α -induced effects, we examined the local expression of VEGF, Akt, and eNOS. Previous studies established a role of NO in EPC podokinesis²⁸ (detachment of EPCs from bone marrow stromal cells), mobilization, and differentiation into endothelial cells in ischemic tissues.²⁹ Both Akt and eNOS are located downstream of VEGF-induced neovascularization.^{30,31} The present results demonstrated that SDF-1 α gene transfer did not affect ischemia-induced enhancement of VEGF expression but did enhance Akt and eNOS activity. VEGF upregulation was localized mainly in ischemic muscles, whereas activation of Akt and eNOS occurred in endothelial cells, implying that interaction of endogenous VEGF from ischemic muscles with endothelial Akt and eNOS is required for SDF-1 α -induced enhancement of ischemic neovascularization. We also demonstrated that the enhanced expression of Akt and eNOS was suppressed by treatment with a VEGF inhibitor, an NOS inhibitor, and their combination. Furthermore, SDF-1-induced neovascularization and EPC mobilization were not observed in eNOS^{-/-} mice. Upregulation of Akt and eNOS might result partly from increased EPC mobilization and neovascularization. Nevertheless, these data suggest that the increased expression and function of VEGF with subsequent activation of Akt and eNOS were involved, at least in part, in the mechanisms by which SDF-1 α enhanced ischemia-induced neovascularization.

Because EPCs express functional CXCR4 and VEGF receptors,^{17,21} an interaction between the SDF-1 α /CXCR4 pathway and VEGF might form a positive-feedback loop to further enhance therapeutic neovascularization in vivo. The present study might have significant clinical implications in that SDF-1 α gene transfer has therapeutic potential for enhancing ischemia-induced neovascularization, at least in part, by mobilizing EPCs to ischemic tissues. More research is required, however, on the effect of SDF-1 α on atherogenesis before translational clinical research begins. SDF-1 α is expressed in human atherosclerotic plaques³² and elicits proinflammatory and platelet-activating actions of SDF-1 α in vitro, suggesting SDF-1 α /CXCR4 inhibition as a therapeutic means for atherosclerosis and acute coronary syndrome.^{33,34} In contrast, anti-inflammatory and plaque-stabilizing effects of SDF-1 α are reported in vitro. Damas et al³⁵ reported that SDF-1 α (500 ng/mL) reduced the release of monocyte chemoattractant protein-1, interleukin-8, matrix metalloproteinases, and tissue factor in peripheral circulating mononuclear cells from patients with unstable angina. More recently,

Schober et al³⁶ reported that SDF-1 α is essential in neointimal formation after vascular injury associated with increased neointimal smooth muscle content. These studies support the concept that therapeutic interventions that enhance SDF-1 α activity could be beneficial in atherosclerotic vascular disease. Therefore, further studies are needed to establish the role of SDF-1 α in the process of atherosclerosis in vivo.

In conclusion, SDF-1 α gene transfer enhanced ischemia-induced vasculogenesis and angiogenesis in vivo through the VEGF/eNOS-related pathway, suggesting that this strategy might be used for the development of a next-generation chemokine therapy for therapeutic neovascularization. This mode of gene therapy might be a novel stand-alone or adjunctive approach for therapeutic neovascularization.

Acknowledgments

This study was supported by Grants-in-Aid for Scientific Research (11470164, 11158216, and 11557056) from the Ministry of Education, Science, and Culture and by Health Science Research Grants (Comprehensive Research on Aging and Health, and Research on Gene Therapy) from the Ministry of Health Labor and Welfare, Tokyo, Japan. We thank Makiko Jichu for assistance with flow cytometry and immunostaining in this study.

References

1. Kerbel R, Folkman J. Clinical translation of angiogenesis inhibitors. *Nat Rev Cancer*. 2002;2:727-739.
2. Schaper W, Scholz D. Factors regulating arteriogenesis. *Arterioscler Thromb Vasc Biol*. 2003;23:1143-1151.
3. Asahara T, Murohara T, Sullivan A, et al. Isolation of putative progenitor endothelial cells for angiogenesis. *Science*. 1997;275:964-967.
4. Asahara T, Masuda H, Takahashi T, et al. Bone marrow origin of endothelial progenitor cells responsible for postnatal vasculogenesis in physiological and pathological neovascularization. *Circ Res*. 1999;85:221-228.
5. Murohara T, Ikeda H, Duan J, et al. Transplanted cord blood-derived endothelial precursor cells augment postnatal neovascularization. *J Clin Invest*. 2000;105:1527-1536.
6. Kamihata H, Matsubara H, Nishiue T, et al. Improvement of collateral perfusion and regional function by implantation of peripheral blood mononuclear cells into ischemic hibernating myocardium. *Arterioscler Thromb Vasc Biol*. 2002;22:1804-1810.
7. Assmus B, Schachinger V, Teupe C, et al. Transplantation of Progenitor Cells and Regeneration Enhancement in Acute Myocardial Infarction (TOPCARE-AMI). *Circulation*. 2002;106:3009-3017.
8. Tateishi-Yuyama E, Matsubara H, Murohara T, et al. Therapeutic angiogenesis for patients with limb ischaemia by autologous transplantation of bone-marrow cells: a pilot study and a randomised controlled trial. *Lancet*. 2002;360:427-435.
9. Inaba S, Egashira K, Komori K. Peripheral-blood or bone-marrow mononuclear cells for therapeutic angiogenesis? *Lancet*. 2002;360:2083; author reply 2084.
10. Vasa M, Fichtlscherer S, Aicher A, et al. Number and migratory activity of circulating endothelial progenitor cells inversely correlate with risk factors for coronary artery disease. *Circ Res*. 2001;89:E1-E7.
11. Hill JM, Zalos G, Halcox JP, et al. Circulating endothelial progenitor cells, vascular function, and cardiovascular risk. *N Engl J Med*. 2003;348:593-600.
12. Iwaguro H, Yamaguchi J, Kalka C, et al. Endothelial progenitor cell vascular endothelial growth factor gene transfer for vascular regeneration. *Circulation*. 2002;105:732-738.
13. Tashiro K, Tada H, Heilker R, et al. Signal sequence trap: a cloning strategy for secreted proteins and type I membrane proteins. *Science*. 1993;261:600-603.
14. Nagasawa T, Kikutani H, Kishimoto T. Molecular cloning and structure of a pre-B-cell growth-stimulating factor. *Proc Natl Acad Sci U S A*. 1994;91:2305-2309.
15. Mohle R, Bautz F, Rafii S, et al. The chemokine receptor CXCR-4 is expressed on CD34+ hematopoietic progenitors and leukemic cells and

- mediates transendothelial migration induced by stromal cell-derived factor-1. *Blood*. 1998;91:4523–4530.
16. Jo DY, Rafii S, Hamada T, et al. Chemotaxis of primitive hematopoietic cells in response to stromal cell-derived factor-1. *J Clin Invest*. 2000;105:101–111.
 17. Salcedo R, Wasserman K, Young HA, et al. Vascular endothelial growth factor and basic fibroblast growth factor induce expression of CXCR4 on human endothelial cells: in vivo neovascularization induced by stromal-derived factor-1 α . *Am J Pathol*. 1999;154:1125–1135.
 18. Aiuti A, Webb IJ, Bleul C, et al. The chemokine SDF-1 is a chemoattractant for human CD34+ hematopoietic progenitor cells and provides a new mechanism to explain the mobilization of CD34+ progenitors to peripheral blood. *J Exp Med*. 1997;185:111–120.
 19. Peled A, Petit I, Kollet O, et al. Dependence of human stem cell engraftment and repopulation of NOD/SCID mice on CXCR4. *Science*. 1999;283:845–848.
 20. Hattori K, Heissig B, Tashiro K, et al. Plasma elevation of stromal cell-derived factor-1 induces mobilization of mature and immature hematopoietic progenitor and stem cells. *Blood*. 2001;97:3354–3360.
 21. Yamaguchi J, Kusano KF, Masuo O, et al. Stromal cell-derived factor-1 effects on ex vivo expanded endothelial progenitor cell recruitment for ischemic neovascularization. *Circulation*. 2003;107:1322–1328.
 22. Masaki I, Yonemitsu Y, Yamashita A, et al. Angiogenic gene therapy for experimental critical limb ischemia: acceleration of limb loss by overexpression of vascular endothelial growth factor 165 but not of fibroblast growth factor-2. *Circ Res*. 2002;90:966–973.
 23. Egashira K, Zhao Q, Kataoka C, et al. Importance of monocyte chemoattractant protein-1 pathway in neointimal hyperplasia after periarterial injury in mice and monkeys. *Circ Res*. 2002;90:1167–1172.
 24. Zhao Q, Egashira K, Inoue S, et al. Vascular endothelial growth factor is necessary in the development of arteriosclerosis by recruiting/activating monocytes in a rat model of long-term inhibition of nitric oxide synthesis. *Circulation*. 2002;105:1110–1115.
 25. Goldman CK, Kendall RL, Cabrera G, et al. Paracrine expression of a native soluble vascular endothelial growth factor receptor inhibits tumor growth, metastasis, and mortality rate. *Proc Natl Acad Sci U S A*. 1998;95:8795–8800.
 26. Jackson KA, Majka SM, Wang H, et al. Regeneration of ischemic cardiac muscle and vascular endothelium by adult stem cells. *J Clin Invest*. 2001;107:1395–1402.
 27. Usui M, Egashira K, Ohtani K, et al. Anti-monocyte chemoattractant protein-1 gene therapy inhibits restenotic changes (neointimal hyperplasia) after balloon injury in rats and monkeys. *FASEB J*. 2002;16:1838–1840.
 28. Noiri E, Lee E, Testa J, et al. Podokinesis in endothelial cell migration: role of nitric oxide. *Am J Physiol*. 1998;274:C236–C244.
 29. Sata M, Nishimatsu H, Suzuki E, et al. Endothelial nitric oxide synthase is essential for the HMG-CoA reductase inhibitor cerivastatin to promote collateral growth in response to ischemia. *FASEB J*. 2001;15:2530–2532.
 30. Ziche M, Morbidelli L, Choudhuri R, et al. Nitric oxide synthase lies downstream from vascular endothelial growth factor-induced but not basic fibroblast growth factor-induced angiogenesis. *J Clin Invest*. 1997;99:2625–2634.
 31. Dimmeler S, Fleming I, Fisslthaler B, et al. Activation of nitric oxide synthase in endothelial cells by Akt-dependent phosphorylation. *Nature*. 1999;399:601–605.
 32. Abi-Younes S, Sauty A, Mach F, et al. The stromal cell-derived factor-1 chemokine is a potent platelet agonist highly expressed in atherosclerotic plaques. *Circ Res*. 2000;86:131–138.
 33. Gupta SK, Pillarisetti K, Lysko PG. Modulation of CXCR4 expression and SDF-1 α functional activity during differentiation of human monocytes and macrophages. *J Leukoc Biol*. 1999;66:135–143.
 34. Gear AR, Camerini D. Platelet chemokines and chemokine receptors: linking hemostasis, inflammation, and host defense. *Microcirculation*. 2003;10:335–350.
 35. Damas JK, Waehre T, Yndestad A, et al. Stromal cell-derived factor-1 α in unstable angina: potential antiinflammatory and matrix-stabilizing effects. *Circulation*. 2002;106:36–42.
 36. Schober A, Knarren S, Lietz M, et al. Crucial role of stromal cell-derived factor-1 α in neointima formation after vascular injury in apolipoprotein E-deficient mice. *Circulation*. 2003;108:2491–2497.

Critical Role of Monocyte Chemoattractant Protein-1 Receptor CCR2 on Monocytes in Hypertension-Induced Vascular Inflammation and Remodeling

Minako Ishibashi, Ken-ichi Hiasa, Qingwei Zhao, Shujiro Inoue, Kisho Ohtani, Shiro Kitamoto, Miyuki Tsuchihashi, Takeshi Sugaya, Israel F. Charo, Shinobu Kura, Teruhisa Tsuzuki, Tatsuro Ishibashi, Akira Takeshita, Kensuke Egashira

Abstract—Activated monocytes are present in the arterial walls of hypertensive patients and animals. Monocyte chemoattractant protein-1 (MCP-1), which controls monocyte function through its receptor (CCR2), is implicated in hypertensive inflammatory changes in the arterial wall. The role of CCR2 expression on monocytes in hypertension-induced vascular remodeling, however, has not been addressed. We hypothesized that CCR2 on monocytes is critical in hypertension-induced vascular inflammation and remodeling. Hypertension was induced by infusion of angiotensin II (Ang II) into wild-type mice, CCR2-deficient (CCR2^{-/-}) mice, and bone marrow-transferred mice with a leukocyte-selective CCR2 deficiency (BMT-CCR2^{-/-}). In wild-type mice, Ang II increased CCR2 intensity in circulating monocytes, which was prevented by an Ang II type-1 (AT₁) receptor blocker or blunted in AT₁ receptor-deficient mice. Enhanced CCR2 intensity on monocytes was observed in hypertensive patients and rats, and was reduced by treatment with the Ang II receptor blocker, supporting the clinical relevance of the observation in mice. In CCR2^{-/-} and BMT-CCR2^{-/-} mice, Ang II-induced vascular inflammation and vascular remodeling (aortic wall thickening and fibrosis) were blunted as compared with control mice. In contrast, Ang II-induced left ventricular hypertrophy developed in CCR2^{-/-} and BMT-CCR2^{-/-} mice. The present study suggests that CCR2 expression in monocytes has a critical role in vascular inflammation and remodeling in Ang II-induced hypertension, and possibly in other forms of hypertension. (*Circ Res.* 2004;94:1203-1210.)

Key Words: vascular remodeling ■ angiotensin II ■ inflammation ■ leukocytes

Chronic monocyte-mediated inflammation in arterial walls is observed in hypertensive patients and animals.¹⁻³ Recent clinical studies reported that lowering angiotensin II (Ang II) activity is a practical target of therapy for patients with cardiovascular disease.⁴⁻⁶ Ang II mediates reactive oxidative species (ROS) and stimulates the release of cytokines and growth factors (interleukin-6) and the expression of adhesion molecules (vascular cell adhesion molecule-1) and chemokines [monocyte chemoattractant protein-1 (MCP-1)] that mediate arterial wall inflammation.¹⁻³ For example, Ang II can induce monocyte chemotaxis by producing MCP-1 from vascular smooth muscle cells and monocytes through NF- κ B.^{7,8}

MCP-1 is a C-C chemokine that controls monocyte recruitment to the site of inflammation through its receptor, C-C chemokine receptor (CCR) 2.⁹⁻¹¹ The MCP-1/CCR2 pathway appears to be involved in the inflammatory aspect of hyper-

tensive artery disease. MCP-1 and CCR2 expression and activity are enhanced in the arterial walls of hypertensive animals.^{12,13} Furthermore, activation of the MCP-1/CCR2 pathway induces monocyte-mediated inflammation, as well as production of adhesion molecules,¹⁴ inflammatory cytokines,¹⁵ and tissue factor,¹⁶ and stimulates migration of vascular smooth muscle cells, resulting in neointimal hyperplasia or atherosclerosis.¹⁷⁻²⁰ We previously demonstrated that blockade of the MCP-1/CCR2 pathway prevents vascular inflammation and arteriosclerosis in rats made hypertensive by chronic inhibition of nitric oxide synthesis.^{13,21-24} Blockade or abrogation of MCP-1 or CCR2 markedly attenuates the early development of atherosclerosis as well as the progression and destabilization of established lesions in hyperlipidemic mice.^{25-28,29} CCR2-deficient (CCR2^{-/-}) mice display reduced neointimal formation after arterial injury.^{24,30}

Original received September 22, 2003; resubmission received February 11, 2004; revised resubmission received March 22, 2004; accepted March 22, 2004.

From the Department of Cardiovascular Medicine (M.I., K.H., Q.Z., S.I., K.O., S. Kitamoto, M.T., A.T., K.E.) and Department of Medical Biophysics and Radiation Biology (S. Kura, T.T.), Department of Ophthalmology (T.I.), Graduate School of Medical Science, Kyushu University, Fukuoka, Japan; Discovery Research Laboratory (T.S.), Tanabe Seiyaku Co, Ltd, Kashima, Osaka, Japan; and Gladstone Institute of Cardiovascular Disease (I.F.C.), San Francisco, Calif.

Correspondence to Kensuke Egashira, MD, PhD, Department of Cardiovascular Medicine, Graduate School of Medical Science, Kyushu University, 3-1-1, Maidashi, Higashi-ku, Fukuoka 812-8582, Japan. E-mail egashira@cardiol.med.kyushu-u.ac.jp

© 2004 American Heart Association, Inc.

Circulation Research is available at <http://www.circresaha.org>

DOI: 10.1161/01.RES.0000126924.23467.A3

Recently, Bush et al³¹ reported that arterial hypertrophy induced by Ang II-induced hypertension was attenuated in CCR2^{-/-} mice, suggesting that CCR2 is required for arterial hypertrophy induced in Ang II-induced hypertension. Most previous studies investigating the inflammatory aspects of hypertensive vascular disease, however, focused exclusively on stress- or injury-induced local changes in inflammation-driving factors in arterial wall cells. The functional importance of CCR2 expression on monocytes in hypertension-induced inflammation and vascular remodeling, on the other hand, has received little attention. Therefore, the present study tested the hypothesis that (1) CCR2 expressed in circulating monocytes is enhanced in hypertensive animals and patients via stimulation of Ang II type-1 (AT₁) receptors; and (2) CCR2 expressed on circulating monocytes has a critical role in hypertension-induced inflammation and vascular remodeling. To dissect the specific role of CCR2 in monocytes, we used bone marrow cells transplantation (BMT) techniques to create mice with a leukocyte-selective CCR2 deficiency (BMT-CCR2^{-/-} mice) and demonstrated that Ang II-induced inflammation and vascular remodeling were blunted in BMT-CCR2^{-/-} mice as well as in CCR2^{-/-} mice.

Materials and Methods

Experimental Animals

Male wild-type mice (C57BL/6J) and those overexpressing human superoxide dismutase (6-TgN(SOD1)3Cje) (SOD-TG) were purchased from Jackson Laboratory (Bar Harbor, Maine). Male AT₁ receptor-deficient mice (AT₁R-KO) on a C57BL/6J genetic background³² were supplied from Tanabe Seiyaku Inc., Osaka, Japan. CCR2^{-/-} and wild-type (CCR2^{+/+}) mice with the same genetic background (C57BL/6J and 129/svjae hybrids) were supplied from Dr Charo.²⁵ Male CCR2^{-/-} and CCR2^{+/+} mice were age matched for all experiments. All mice were bred and maintained in the Laboratory of Animal Experiments at Kyushu University. Twenty-week-old male Wistar-Kyoto (WKY) rats and 12-week-old spontaneous hypertensive rats (SHR) were obtained from an established colony at the animal Research Institution of Kyushu University, Faculty of Medical Sciences (Fukuoka, Japan).

Experimental Protocol

The study protocol was reviewed and approved by the Committee on the Ethics of Animal Experiments, Kyushu University Graduate School of Medical Sciences. A part of this study was performed at the Kyushu University Station for Collaborative Research and the Morphology Core Unit, Kyushu University Faculty of Medical Sciences.

Experiment 1

To examine whether Ang II affects CCR2 fluorescence intensity in circulating monocytes *in vivo*, Ang II was infused into several groups of 12-week-old wild-type mice treated with or without AT₁ receptor blocker (ARB), AT₁R-KO, or SOD-TG mice. The control group received untreated chow and drinking water. The Ang II group received Ang II via an osmotic minipump (Alzet) (1.9 mg/kg per day). The minipump was implanted in the peritoneal cavity under anesthesia with ketamine (80 mg/kg IP) and xylazine (10 mg/kg IP). The Ang II+ARB groups received Ang II by an osmotic minipump and ARB (olmesartan at 0.35 or 3.5 mg/kg per day) in chow. Olmesartan was a gift from Sankyo Pharmaceutical Co (Tokyo, Japan). Treatment with olmesartan was started 3 days before Ang II administration was begun. The AT₁R-KO+Ang II and SOD-TG+Ang II groups were infused with Ang II by osmotic minipumps.

Experiment 2

To determine the role of CCR2 in Ang II-induced vascular remodeling, four groups of 12-week-old CCR2^{-/-} and CCR2^{+/+} mice infused with Ang II or PBS via osmotic minipump were studied.

Experiment 3

To dissect the specific role of CCR2 in the monocytes, we used the BMT technique to create mice with a leukocyte selective CCR2 deficiency (BMT-CCR2^{-/-}). At 8 weeks of age, BMT was performed as described previously.³³ Bone marrow cells were harvested from femurs and tibias of either test (CCR2^{-/-}) or control (CCR2^{+/+}) donor mice. The recipient CCR2^{+/+} mice received 1×10⁷ bone marrow cells (0.3 mL) 4 hours after whole body irradiation with 7 Gy of X-rays (200 KVp, 20 mA, 0.3 mmCu filter) at 1Gy/min. These two groups of mice are referred to as BMT-CCR2^{-/-} and BMT-CCR2^{+/+}, respectively. Four groups of BMT-CCR2^{-/-} and BMT-CCR2^{+/+} mice infused with Ang II or PBS were studied. BMT-AT₁R-KO mice also were created in a same manner. To ensure that the exposure dose was sufficient to ablate the bone marrow, a group of C57BL/6J mice (n=6) was irradiated and injected with bone marrow cells from C57BL/6J mice expressing green fluorescence protein. Flow cytometric analysis of circulating leukocytes from recipient mice at 4 weeks after transplantation revealed that the chimerism was 95±2%.

Experiment 4

To examine the effect of ARB on monocyte CCR2 fluorescence intensity in other forms of hypertension, we used WKY rats treated with N^ω-nitro-L-arginine methyl ester (L-NAME) and SHR treated with or without ARB.

In all experiments, mice were euthanized on day 3, 7, or 28 of treatment for morphometric, immunohistochemical, and biochemical analysis. Venous blood was collected immediately before the mice were euthanized. The aortas and hearts were isolated and either fixed in 10% buffered formalin for histologic analysis or snap-frozen in liquid nitrogen and stored at -80°C for biochemical analysis. Systolic blood pressure was measured by the tail-cuff method before and 3, 7, and 28 days after treatment.

Histology and Immunohistochemistry

Histopathology and immunohistochemistry were performed as described previously.^{24,28} Some sections were subjected to immunostaining using antibodies against mouse macrophages (Mac-3, Serotec Inc), proliferating cell nuclear antigen (PCNA, DAKO), α -smooth muscle cell actin (α -SM actin) (Boehringer Mannheim), MCP-1, and CCR2 (Santa Cruz Biotechnology Inc). The degree of vascular remodeling (the medial thickness and perivascular fibrosis of aorta) and left ventricular hypertrophy [left ventricular to body weight ratios (LV/BW)] on day 28 was measured as described previously.²³

TaqMan Real-Time Reverse Transcription-Polymerase Chain Reaction Analysis

TaqMan real-time reverse transcription-polymerase chain reaction (RT-PCR) was performed as previously described.¹⁸ Transcripts from 1 μ g total RNA were reverse-transcribed and the resultant cDNA was amplified by TaqMan real-time RT-PCR. The PCR primers for mouse MCP-1, CCR2, and B-type natriuretic peptide (BNP) were sense primer 5'-CCTGGATCGGA-ACCAAATGA-3', antisense primer 5'-CGGGTCAACTTCA-CATTCAAAG-3', and probe oligonucleotides 5'-AACT-GCATCTGCCCTAAGG-TCTTCAGCA-3' for MCP-1, and sense primer 5'-CCTTGGGA-ATGAGTAACTGTGTGAT-3', antisense primer 5'-ATGGA-GAGATACCTTCGGAACCTCT-3', and probe oligonucleotides 5'-CACTTAGACCAGGCCATGCAGGT-GACA-3' for CCR2, and sense primer 5'-GCCAGTCTCCAG-AGCAATTCA-3', antisense primer 5'-GTGAGGCCTTGG-TCCTTCAA-3', and probe oligonucleotides 5'-TCTCTTATCA-GCTCCAGCAGCTTCTGCA-3' for BNP. GAPDH probe was obtained from Applied Biosystems.

Flow Cytometry Analysis

Flow cytometry analysis was performed as described previously.³³ To determine CCR2 expression in monocytes, isolated leukocytes were stained using antibodies against phycoerythrin (PE)-conjugated anti-mouse monocyte (CD80) (Becton Dickinson Biosciences), goat anti-mouse CCR2 (Santa Cruz Biotechnology Inc), and FITC-conjugated mouse anti-goat IgG (Santa Cruz Biotechnology Inc.). To determine CCR2 fluorescence intensity in lymphocytes and neutrophils, leukocytes were also stained using antibodies against PE-conjugated anti-mouse CD11b (Mac-1), cy-chrome-conjugated anti-mouse T-cell receptor β chain monoclonal antibody (Becton Dickinson Biosciences). In control experiments, FITC-conjugated nonspecific goat IgG was used to measure nonspecific binding. The fluorescent probe, 2',7',-dichlorofluorescein diacetate (DCFH-DA, Molecular Probes Inc), was used to detect intracellular ROS. Isolated leukocytes were stained using DCFH-DA and PE-conjugated anti-mouse CD80 for 30 minutes at 4°C. Stained cells were analyzed by FACSCalibur (Becton Dickinson Biosciences).

Peripheral Blood Mononuclear Cell Chemotaxis

Mouse mononuclear cells were purified by centrifugation on Lympholyte-M and were washed with RPMI 1640. Cell migration was measured in 96-well chemotaxis chambers (Neuro Probe Inc). MCP-1 in RPMI 1640 (25 ng/mL) was added to the lower and the isolated mononuclear cells (2×10^7) in the same medium to the upper wells. After incubation for 90 minutes at 37°C, the membrane was removed, washed on the upper side with PBS. Migrated cells were counted. All assays were performed in triplicate.

Plasma Measurements

Commercially available ELISA kits (Biosource International) were used to measure mouse MCP-1 according to the manufacturer's instructions.

Patient Studies

Patients with hypertension who had no other evidence of other cardiovascular disease, infectious disease, inflammatory disorders, connective tissue disease, or prior malignant tumor disease, were enrolled. The patients were divided into three groups: normotensive group (systolic/diastolic blood pressure <140/90 mm Hg), untreated essential hypertensive patients (systolic/diastolic blood pressure \geq 140/90 mm Hg), and hypertensive patients treated solely with ARB (losartan, candesartan, and valsartan). Hypertensive patients treated with a combination of antihypertensive drugs were not enrolled. Written informed consent was obtained from all patients.

Blood samples were obtained from all patients in the fasting state. White blood cell count, C-reactive protein, and plasma lipid, as well as plasma MCP-1 (human MCP-1 ELISA kit, Biosource International) were measured. The fluorescence intensity of chemokine receptors on leukocytes (the MCP-1 receptor CCR2 on monocytes, the interleukin-8 receptor CXCR2 on neutrophils, and the RANTES receptor CCR1 on T cells, DAKO) also was assessed by flow cytometry.

There were no significant differences in age, body mass index, plasma lipid levels, white blood cell count, or smoking habit among groups (Table 1). Plasma concentrations of MCP-1 and C-reactive protein were lower in the ARB-treated group, although the difference was not statistically significant. As expected, systolic and diastolic blood pressure were significantly higher in untreated hypertensive patients than in normotensive control subjects. Blood pressure values were lower in hypertensive patients treated with ARB than in untreated hypertensive patients, although the difference was not statistically significant. Hypertensive patients treated with ARB had a significantly higher proportion of diabetes mellitus.

Statistical Analysis

Data are expressed as mean \pm SE. In animal studies, statistical analysis of differences was compared by ANOVA using Bonferroni's correction for multiple comparisons. In human studies, multiple logistic regression analysis was performed to identify significant

TABLE 1. Clinical and Biochemical Characteristics of Hypertensive Patients With and Without ARB Treatment and Normotensive Controls

Variables	Normotensive Controls n=40	Untreated HT n=30	HT Treated With ARB n=30
Age	55 \pm 12	63 \pm 8	59 \pm 11
Male, %	71.7	63.0	63.6
Smoking, %	23.9	40.7	37.3
Body mass index	23 \pm 3	24 \pm 4	23 \pm 3
Hypercholesterolemia, %	34.8	37.0	46.4
Diabetes, %	21.1	29.6	53.7*
Systolic BP, mm Hg	115 \pm 12	151 \pm 10*	143 \pm 17*
Diastolic BP, mm Hg	67 \pm 10	84 \pm 9*	81 \pm 10*
WBC, $\times 10^9/\mu$ L	5.5 \pm 1.6	5.9 \pm 1.6	5.4 \pm 2.0
Monocyte count, $\times 10^9/\mu$ L	314 \pm 116	302 \pm 115	262 \pm 122
Total cholesterol, mg/dL	205 \pm 43	203 \pm 36	216 \pm 37
Triglycerides, mg/dL	120 \pm 57	119 \pm 50	142 \pm 53
LDL-C, mg/dL	112 \pm 33	108 \pm 34	114 \pm 21
C-reactive protein, mg/dL	0.13 \pm 0.4	0.17 \pm 0.3	0.10 \pm 0.3
MCP-1, pg/mL	11 \pm 6	13 \pm 10	9 \pm 6
CCR2 in monocytes, MFI	115 \pm 32	168 \pm 37*	111 \pm 24†
CXCR2 in neutrophils, MFI	85 \pm 35	77 \pm 25	81 \pm 16
CCR1 on T cells, MFI	10 \pm 3	11 \pm 3	10 \pm 3

Values are mean \pm SEM. * P <0.01 vs normotensive controls, † P <0.01 vs untreated hypertensive patients (HT).

independent predictors of the presence of hypertension. Odds ratio and 95% confidence intervals were calculated. A level of P <0.05 was considered statistically significant.

Results

Ang II-Induced Upregulation of CCR2 in Circulating Monocytes in Wild-Type Mice

Flow-cytometry analysis indicated that monocyte CCR2 intensity peaked on day 7 and the higher level was sustained until day 28 of Ang II infusion (Figure 1A). The Ang II-induced increase in CCR2 intensity on day 7 was prevented by treatment with low and high doses of ARB. The Ang II-induced increase in CCR2 intensity was blunted in AT₁R-KO, SOD-TG, and BMT-AT₁R-KO mice (Figure 1B). No CCR2 antigen was detected on lymphocytes or neutrophils in the presence or absence of Ang II infusion. To determine the functional role of the CCR2 upregulation in monocytes, chemotaxis assay was performed in peripheral blood mononuclear cells. No chemotactic response was detected in monocytes from control untreated mice. In contrast, MCP-1-mediated chemotaxis was increased in monocytes from mice infused Ang II for 7 days, which was blunted in monocytes from CCR2^{-/-} mice (Figure 1C). These chemotaxis data are in agreement with previous studies by other investigators^{34,35} that the measured increase in CCR2 intensity on monocytes resulted in increased monocyte chemotaxis in response to MCP-1.

To study the effects of Ang II on intracellular ROS, intracellular ROS were measured in monocytes by

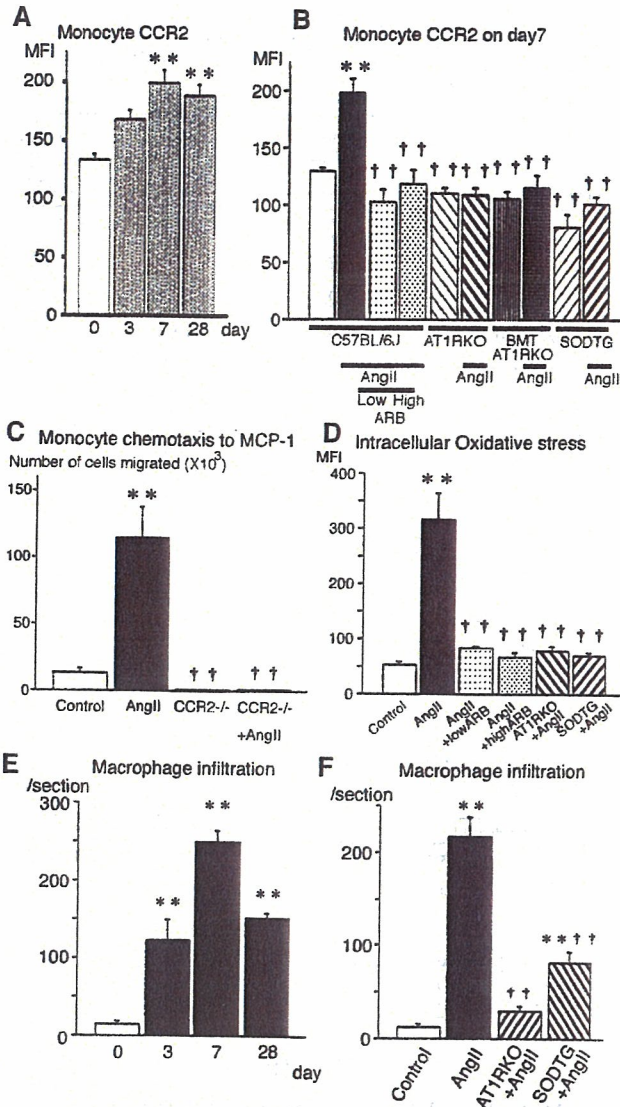


Figure 1. Ang II-induced CCR2 expression on circulating monocytes and macrophage infiltration into the aorta in wild-type mice. **A**, Time course of mean fluorescence intensity (MFI) of CCR2 on the surface of the circulating monocytes; n=6 to 8. **B**, Effects of ARB, AT₁ deficiency, leukocyte-selective AT₁R deficiency, and SOD overexpression on Ang II-induced enhancement of CCR2 expression on day 7; n=7 each. **C**, Effects of increased CCR2 expression on peripheral mononuclear cells chemotaxis in response to MCP-1 (25 ng/mL) in wild-type and CCR2^{-/-} mice infused with or without Ang II for 7 days. **D**, Effects of ARB, AT₁ deficiency, and SOD overexpression on intracellular production of ROS in monocytes; n=6 each. **E**, Time course of macrophage infiltration after Ang II infusion (number of Mac-3-positive macrophages per section); n=6 each. **F**, Effect of ARB, AT₁ deficiency, and SOD overexpression on Ang II-induced macrophage infiltration into the aorta. Number of Mac-3-positive macrophages per section was determined on day 7; n=6 each. *P<0.05, **P<0.01 vs control group; †P<0.05, ††P<0.01 vs Ang II group.

DCFH-DA fluorescence intensity (Figure 1D). Levels of ROS were undetectable in monocytes from untreated control mice, but were significantly increased in monocytes from mice infused with Ang II for 7 days. Treatment with the low and high doses of ARB prevented the increase in intracellular

ROS. The Ang II-induced increase in ROS was blunted in AT₁R-KO and SOD-TG mice.

The time course of macrophages infiltration into the aorta was similar to that of monocyte CCR2 expression after Ang II infusion (Figures 1E and 1F). There was reduced Ang II-induced monocyte infiltration into the aorta in mice treated with low and high doses of ARB, AT₁R-KO, and SOD-TG mice.

Compared with the control group, Ang II infusion induced a rise in systolic blood pressure (online Table 1, available in the online data supplement at <http://circres.ahajournals.org>). Similar changes in blood pressure were observed in Ang II+Low ARB and SOD-TG+Ang II groups. No Ang II-induced increase in blood pressure was observed in the Ang II+High ARB and AT₁R-KO+Ang II groups (online Table 2). Baseline blood pressure was lower in AT₁R-KO mice, although the difference was not statistically significant.

Ang II-Induced Upregulation of MCP-1 and CCR2 in the Aorta in Wild-Type Mice

As previously reported,^{12,31} Ang II infusion to wild-type mice for 7 days increased mRNA levels of MCP-1 and CCR2 (Figure 2A). Treatment with low and high doses of ARB prevented the increased gene expression. The Ang II-induced increase in gene expression was blunted in AT₁R-KO and SOD-TG mice. Immunohistochemical staining indicated that Ang II infusion increased MCP-1 in lesional macrophages on days 3 and 7, and the increase was sustained until day 28 (Figures 2B and 2C). Increased MCP-1 staining was noted in smooth muscle cells of the media on day 28. Increased CCR2 staining was observed in infiltrating macrophages on days 3, 7, and 28. Treatment with low and high doses of ARB prevented the Ang II-induced increase in immunostaining for MCP-1 and CCR2 (data not shown).

Inhibition of Ang II-Induced Vascular Remodeling in CCR2^{-/-} Mice

As previously reported,³¹ Ang II infusion to CCR2^{+/+} mice for 7 days induced infiltration of Mac-3-positive macrophages into the aortic wall, mainly into the adventitia (Figure 3A). PCNA-positive proliferating cells appeared in cells in the endothelial layer, media, and adventitia. There were also α-SM actin-positive cells (myofibroblast) in the adventitia of Ang II-infused wild-type mice (data not shown). On day 28, aortic remodeling (medial wall thickening and perivascular fibrosis) developed in CCR2^{+/+} mice. In contrast, aortic inflammatory-proliferative changes in the early stage and vascular remodeling in the late stage were markedly attenuated in CCR2^{-/-} mice (Figure 3B).

There were no significant differences in plasma MCP-1 levels between untreated CCR2^{+/+} and CCR2^{-/-} mice on day 28 (online Table 2). In contrast, the plasma MCP-1 level dramatically increased in CCR2^{-/-} mice infused with Ang II, compared with that in CCR2^{+/+} mice infused with Ang II.

There were no significant differences in Ang II-induced changes in systolic blood pressure or left ventricular hypertrophy (online Table 2).

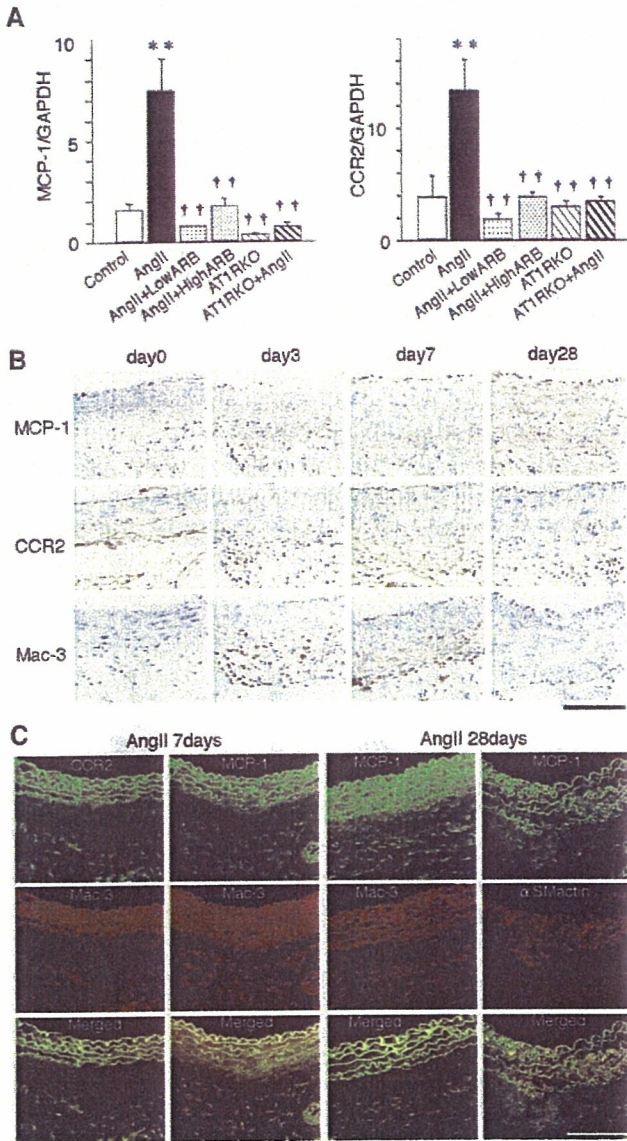


Figure 2. Ang II-induced expression of MCP-1 and CCR2 in the aorta in wild-type mice. **A**, MCP-1 and CCR2 gene expression by real-time RT-PCR in the aorta. Data are expressed as the ratio of MCP-1 and CCR2 mRNA to GAPDH mRNA. * $P < 0.05$, ** $P < 0.01$ vs control group; † $P < 0.05$, †† $P < 0.01$ vs Ang II group; $n = 6$ each. **B**, Aortic cross sections were stained immunohistochemically for MCP-1, CCR2, and macrophage (Mac-3) on days 0, 3, 7, and 28 ($n = 6$ each) (bar = 100 μm). **C**, Immunofluorescence double staining of aorta using anti-mouse CCR2, MCP-1, Mac-3, or α -SM actin antibody. CCR2 and MCP-1 immunofluorescence (labeled green with FITC), Mac-3 and α -SM actin immunofluorescence (labeled red with rhodamine), and their merged images (yellow) are presented. Background nonspecific fluorescence is observed in elastic layers of aortas (bar = 100 μm).

Blunted Ang II-Induced Vascular Remodeling in BMT-CCR2^{-/-} Mice

There were no differences in the degree of aortic wall thickening or perivascular fibrosis between untreated BMT-CCR2^{+/+} and BMT-CCR2^{-/-} mice. BMT-CCR2^{+/+} mice developed significant vascular remodeling and left ventricular hypertrophy in response to Ang II infusion to an extent similar to that in nonirradiated CCR2^{+/+} mice. In contrast, Ang II-induced aortic wall thickening and perivascular fibro-

sis were blunted in BMT-CCR2^{-/-} mice (Figures 4A and 4B). There were no significant differences in Ang II-induced hypertension, left ventricular hypertrophy, or the increase in BNP mRNA levels between BMT-CCR2^{+/+} and BMT-CCR2^{-/-} mice (online Table 3).

As in nonirradiated CCR2^{-/-} mice, there was a significant increase in plasma MCP-1 levels only in BMT-CCR2^{-/-} mice infused with Ang II (online Table 3). Ang II-induced increases in MCP-1 mRNA and immunoreactive MCP-1 levels in the aorta were also similar between BMT-CCR2^{+/+} and BMT-CCR2^{-/-} mice (Figure 5). Aortic CCR2 gene expression was blunted in BMT-CCR2^{-/-} mice infused with and

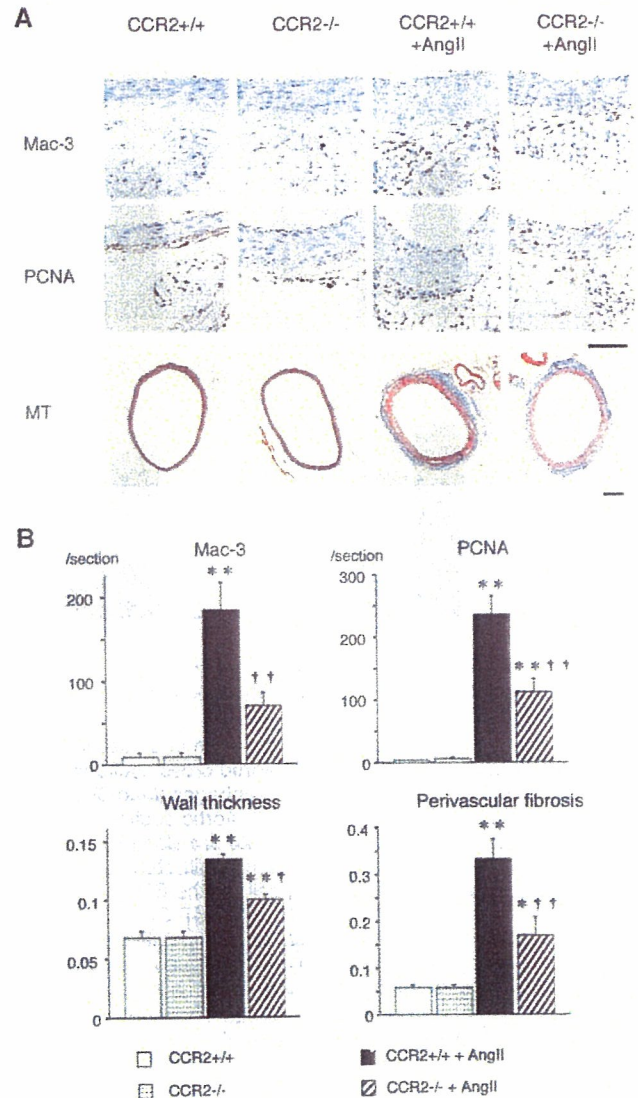


Figure 3. Inhibition of Ang II-induced inflammation and vascular remodeling in CCR2^{-/-} mice. **A**, Aortic cross sections were immunohistochemically stained for macrophages (Mac-3) or a marker of proliferation (PCNA) on day 7. Aortic sections stained with Masson's trichrome on day 28 are also shown (bar = 100 μm). **B**, Number of macrophages infiltrated into the aorta and appearance of proliferating cells in the CCR2^{+/+}, CCR2^{-/-}, CCR2^{+/+}+Ang II, and CCR2^{-/-}+Ang II mice on day 7 of Ang II infusion are shown (positive cell counts per section). Wall thickness (wall-to-lumen ratio) and perivascular fibrosis of aorta on day 28 are shown. * $P < 0.05$, ** $P < 0.01$ vs CCR2^{+/+} group; † $P < 0.05$, †† $P < 0.01$ vs CCR2^{+/+}+Ang II group ($n = 6$ each).

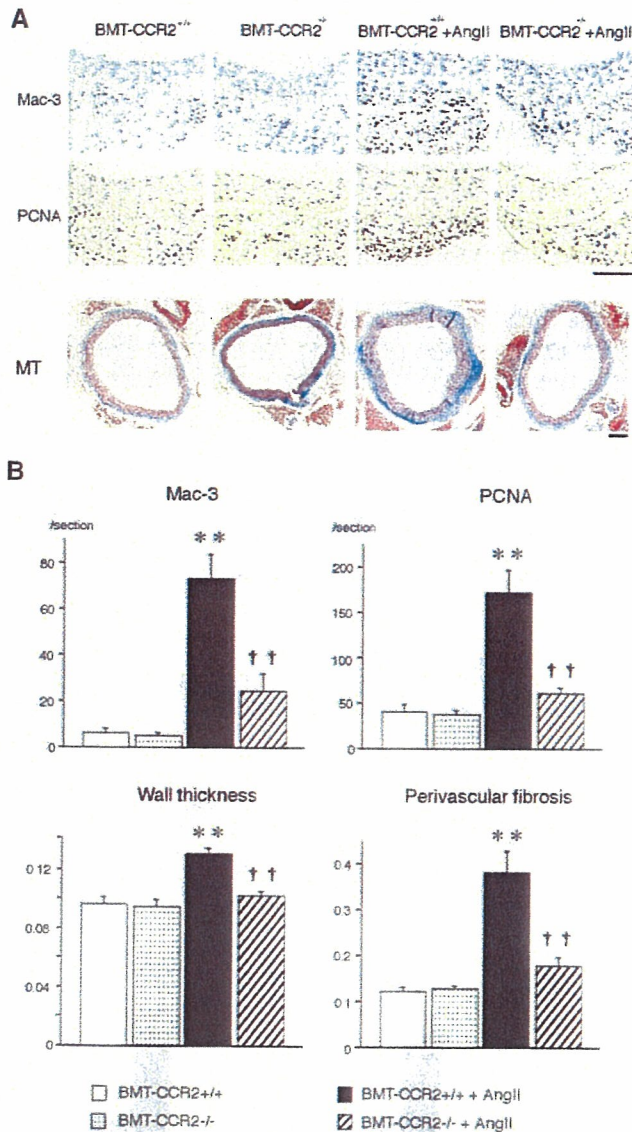


Figure 4. Blunted Ang II-induced inflammation and vascular remodeling in BMT-CCR2^{-/-} mice. A, Aortic cross sections were immunohistochemically stained for macrophages (Mac-3) or a marker of proliferation (PCNA) on day 28. Aortic sections stained with Masson's trichrome on day 28 are also presented (bar=100 μm). B, Number of macrophages infiltrated into the aorta and appearance of proliferating cells in the BMT-CCR2^{+/+}, BMT-CCR2^{-/-}, BMT-CCR2^{+/+}+Ang II, and BMT-CCR2^{-/-}+Ang II mice of day 28 of Ang II infusion are shown (positive cell counts per section). Wall thickness (wall-to-lumen ratio) and perivascular fibrosis of the aorta on day 28 are also shown. **P*<0.05, ***P*<0.01 vs BMT-CCR2^{+/+} group; †*P*<0.05, ††*P*<0.01 vs BMT-CCR2^{+/+}+Ang II group (n=6 each).

without Ang II, suggesting that lesional macrophages might be the major source of CCR2 gene expression in the aortic tissue.

Effects of ARB on CCR2 Expression in Circulating Monocytes in Hypertensive Patients

A pilot clinical study was performed to determine if monocyte CCR2 is enhanced in patients with essential hypertension via AT₁ receptor stimulation. Multivariate analysis revealed that the increased CCR2 intensity on monocytes

correlated independently with the presence of hypertension (odds ratio=33.6, 95% confidence interval=4.22~267.5; *P*<0.01; Table 2). The monocyte CCR2 intensity in hypertensive patients treated with ARB was similar to that observed in normotensive subjects (Table 1). There were no significant differences in monocyte CCR2 levels in patients treated with different ARB (data not shown). In contrast, there were no significant differences in CXCR2 in neutrophils, or CCR1 in T cells among the three groups (Table 1). There was no significant correlation between the CCR2 intensity on monocytes and the degree of systolic or diastolic hypertension (data not shown).

CCR2 Upregulation in Peripheral Circulating Monocytes of Hypertensive Rats

Monocyte CCR2 intensity was higher in WKY rats made hypertensive with administration of the nitric oxide synthesis inhibitor (L-NAME) for 1 week²³ compared with control

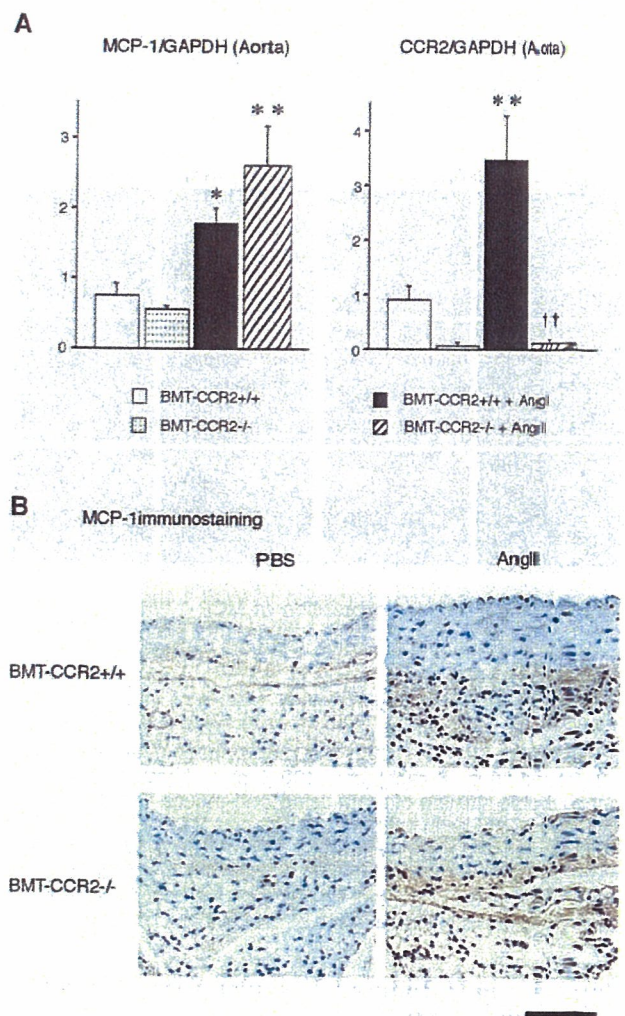


Figure 5. MCP-1 and CCR2 expression of the aorta in BMT mice. A, MCP-1 and CCR2 gene expression by real-time RT-PCR in the aorta on day 28. Data are expressed as the ratio of MCP-1 and CCR2 mRNA to GAPDH mRNA. **P*<0.05, ***P*<0.01 vs BMT-CCR2^{+/+} group; †*P*<0.05, ††*P*<0.01 vs BMT-CCR2^{+/+}+Ang II group (n=6 each). B, Aortic cross sections were stained immunohistochemically for MCP-1 on day 28 (bar=100 μm).

TABLE 2. Identification of Independent Predictors of the Presence of Hypertension by Multivariate Analysis

Variables	Odds Ratio	95% CI	P
Nonpredictor			
Sex, male	6.02	0.77–47.4	0.40
Age, >70 years	2.24	0.26–19.5	0.47
Smoking	3.49	0.41–29.5	0.25
Alcohol	0.80	0.11–5.82	0.83
Body mass index, >25	6.46	0.55–75.2	0.14
Hypercholesterolemia			
TC, >220 mg/dL	0.28	0.03–2.63	0.26
HDL-C, <40 mg/dL	0.37	0.44–3.51	0.39
LDL-C, >130 mg/dL	0.88	0.07–11.3	0.92
Diabetes	1.78	0.18–17.9	0.63
MCP-1, <8 ng/mL	0.54	0.10–3.04	0.49
CXCR2/neutrophils, MFI	0.98	0.94–1.01	0.15
CCR2/T cells, MFI	0.99	0.74–1.32	0.95
Predictor			
CCR2/monocytes, >130, MFI	33.6	4.22–267.5	<0.01

untreated rats. The increase in monocyte CCR2 intensity was prevented by treatment with low and high doses of ARB. Monocyte CCR2 intensity was also enhanced in 12-week old SHR, which was reduced by treatment with low and high doses of ARB (online Table 4).

Discussion

Hypertension-induced mechanical strains on monocytes and endothelial cells activate monocyte function resulting in hyperresponsiveness to inflammatory stimuli and secretion of cytokines and growth factors.^{36–38} The novel findings of the present study are that (1) CCR2 expression and function (chemotaxis to MCP-1) are enhanced in circulating monocytes in hypertensive animals through an AT₁ receptor-mediated mechanism, and (2) monocyte CCR2 is critical for monocyte-mediated inflammation and remodeling in Ang II-induced hypertension in mice. Although the precise molecular mechanism underlying AT₁ receptor-mediated overexpression of CCR2 in the monocytes is not known, the present data using the SOD-TG mice suggest the possible involvement of ROS. The involvement of ROS is supported by a recent report by Wang et al³⁵ who demonstrated that treatment of isolated monocytes with antioxidants reduced homocysteine-induced increases in CCR2.

The pilot clinical study indicating that (1) increased CCR2 on monocytes is an important predictor of the presence of hypertension, and (2) hypertensive patients treated with ARB have reduced levels of monocyte CCR2 suggests potential clinical implications of the present observation in animals. Our present data of (1) identical effects of treatment with low and high doses of ARB on monocyte CCR2 expression in mice and rats, and (2) no significant correlation between blood pressure values and the monocyte CCR2 intensity in patients support the hypothesis that ARB-induced diminished CCR2 expression is not explained solely by the blood pressure-lowering effects of ARB. Therefore, a direct action

of Ang II mediated via AT₁ receptors beyond blood pressure lowering might be involved in the pathobiology of enhanced monocyte CCR2 expression and function under hypertensive conditions in vivo.

To dissect the relative pathobiological role of monocytes versus nonmonocyte cells in the arterial wall, we used the BMT technique. The most important finding of this study was blunted Ang II-induced aortic inflammation and remodeling in BMT-CCR2^{-/-} mice as well as in CCR2^{-/-} mice. In contrast, cardiac hypertrophy developed in both CCR2^{-/-} and BMT-CCR2^{-/-} mice. The present study therefore provides direct evidence that increased CCR2 expression on monocytes is critical for the development of vascular inflammation and remodeling, but not for left ventricular hypertrophy, in Ang II-induced hypertension. It is plausible therefore that suppression of Ang II-induced vascular remodeling by leukocyte-selective CCR2 deficiency may be the result of reduced recruitment and activation of monocytes. Activated leukocytes might produce growth-promoting signals, which in turn lead to vascular remodeling in a CCR2-deficiency manner. In contrast, Roque et al³⁰ suggested that upregulation of MCP-1 is responsible for attenuating neointimal smooth muscle growth after arterial injury in CCR2^{-/-} mice. Although there was no detectable difference in Ang II-induced local MCP-1 expression between BMT-CCR2^{+/+} and -CCR2^{-/-} mice, it is possible that some of inhibitory effects seen in BMT-CCR2^{-/-} mice might be related to direct inhibitory effects of MCP-1. The blunted Ang II-induced inflammation and vascular remodeling in BMT-CCR2^{-/-} mice cannot be explained by nonspecific action of irradiation, because (1) Ang II-induced structural changes in the aorta and heart were similar between CCR2^{+/+} and BMT-CCR2^{+/+} mice and (2) Ang II-induced increases in gene and protein expression of MCP-1 were noted in CCR2^{-/-} and BMT-CCR2^{-/-} mice. In conclusion, the present study provides solid evidence that CCR2 expressed on monocytes has a critical role in vascular inflammation and remodeling in Ang II-induced hypertension. This finding might also apply to the pathology of vascular remodeling due to other types of hypertension, because enhanced CCR2 expression and its inhibition by ARB treatment was demonstrated in other types of hypertensive animals and in hypertensive patients. The present data suggest that CCR2-mediated monocyte inflammation is a reasonable target of therapy for treatment of vascular remodeling. Also, blockade of Ang II signals by ARB might act as antiinflammatory therapy beyond blood pressure lowering.

Acknowledgments

This study was supported by Grants-in-Aid for Scientific Research (14657172, 14207036) from the Ministry of Education, Culture, Sports, Science and Technology, Tokyo, Japan, by Health Science Research Grants (Comprehensive Research on Aging and Health, and Research on Translational Research) from the Ministry of Health Labor and Welfare, Tokyo, Japan, and by the Program for Promotion of Fundamental Studies in Health Sciences of the Organization for Pharmaceutical Safety and Research, Tokyo, Japan.

References

1. Dzau VJ. Theodore Cooper lecture. Tissue angiotensin and pathobiology of vascular disease: a unifying hypothesis. *Hypertension*. 2001;37:1047–1052.

2. Alexander RW. Theodore Cooper memorial lecture. Hypertension and the pathogenesis of atherosclerosis: oxidative stress and the mediation of arterial inflammatory response: a new perspective. *Hypertension*. 1995; 25:155–161.
3. Egashira K. Clinical importance of endothelial function in arteriosclerosis and ischemic heart disease. *Circ J*. 2002;66:529–533.
4. Yusuf S, Sleight P, Pogue J, Bosch J, Davies R, Dagenais G. Effects of an angiotensin-converting-enzyme inhibitor, ramipril, on cardiovascular events in high-risk patients: the heart outcomes prevention evaluation study investigators. *N Engl J Med*. 2000;342:145–153.
5. Pitt B, Poole-Wilson PA, Segal R, Martinez FA, Dickstein K, Camm AJ, Konstam MA, Riegger G, Klingler GH, Neaton J, Sharma D, Thiyagarajan B. Effect of losartan compared with captopril on mortality in patients with symptomatic heart failure: randomised trial—the losartan heart failure survival study elite II. *Lancet*. 2000;355:1582–1587.
6. Cohn JN, Tognoni G. A randomized trial of the angiotensin-receptor blocker valsartan in chronic heart failure. *N Engl J Med*. 2001;345:1667–1675.
7. Hernandez-Presa M, Bustos C, Ortego M, Tunon J, Renedo G, Ruiz-Ortega M, Egido J. Angiotensin-converting enzyme inhibition prevents arterial nuclear factor- κ B activation, monocyte chemoattractant protein-1 expression, and macrophage infiltration in a rabbit model of early accelerated atherosclerosis. *Circulation*. 1997;95:1532–1541.
8. Chen XL, Tummala PE, Olbrych MT, Alexander RW, Medford RM. Angiotensin II induces monocyte chemoattractant protein-1 gene expression in rat vascular smooth muscle cells. *Circ Res*. 1998;83:952–959.
9. Gerard C, Rollins BJ. Chemokines and disease. *Nat Immunol*. 2001;2:108–115.
10. Mukaida N, Harada A, Matsushima K. Interleukin-8 (IL-8) and monocyte chemotactic and activating factor (mcaf/mcp-1), chemokines essentially involved in inflammatory and immune reactions. *Cytokine Growth Factor Rev*. 1998;9:9–23.
11. Egashira K. Molecular mechanisms mediating inflammation in vascular disease: special reference to monocyte chemoattractant protein-1. *Hypertension*. 2003;41:834–841.
12. Capers Qt, Alexander RW, Lou P, De Leon H, Wilcox JN, Ishizaka N, Howard AB, Taylor WR. Monocyte chemoattractant protein-1 expression in aortic tissues of hypertensive rats. *Hypertension*. 1997;30:1397–1402.
13. Usui M, Egashira K, Tomita H, Koyanagi M, Katoh M, Shimokawa H, Takeya M, Yoshimura T, Matsushima K, Takeshita A. Important role of local angiotensin II activity mediated via type 1 receptor in the pathogenesis of cardiovascular inflammatory changes induced by chronic blockade of nitric oxide synthesis in rats. *Circulation*. 2000;101:305–310.
14. Jiang Y, Beller DI, Frenzl G, Graves DT. Monocyte chemoattractant protein-1 regulates adhesion molecule expression and cytokine production in human monocytes. *J Immunol*. 1992;148:2423–2428.
15. Viedt C, Vogel J, Athanasiou T, Shen W, Orth SR, Kubler W, Kreuzer J. Monocyte chemoattractant protein-1 induces proliferation and interleukin-6 production in human smooth muscle cells by differential activation of nuclear factor- κ B and activator protein-1. *Arterioscler Thromb Vasc Biol*. 2002;22:914–920.
16. Schechter AD, Rollins BJ, Zhang YJ, Charo IF, Fallon JT, Rossikhina M, Giesen PL, Nemerson Y, Taubman MB. Tissue factor is induced by monocyte chemoattractant protein-1 in human aortic smooth muscle and THP-1 cells. *J Biol Chem*. 1997;272:28568–28573.
17. Mori E, Komori K, Yamaoka T, Tani M, Kataoka C, Takeshita A, Usui M, Egashira K, Sugimachi K. Essential role of monocyte chemoattractant protein-1 in development of restenotic changes (neointimal hyperplasia and constrictive remodeling) after balloon angioplasty in hypercholesterolemic rabbits. *Circulation*. 2002;105:2905–2910.
18. Usui M, Egashira K, Ohtani K, Kataoka C, Ishibashi M, Hiasa K, Katoh M, Zhao Q, Kitamoto S, Takeshita A. Anti-monocyte chemoattractant protein-1 gene therapy inhibits restenotic changes (neointimal hyperplasia) after balloon injury in rats and monkeys. *FASEB J*. 2002;16:1838–1840.
19. Namiki M, Kawashima S, Yamashita T, Ozaki M, Hirase T, Ishida T, Inoue N, Hirata K, Matsukawa A, Morishita R, Kaneda Y, Yokoyama M. Local overexpression of monocyte chemoattractant protein-1 at vessel wall induces infiltration of macrophages and formation of atherosclerotic lesion: synergism with hypercholesterolemia. *Arterioscler Thromb Vasc Biol*. 2002;22:115–120.
20. Aiello RJ, Bourassa PA, Lindsey S, Weng W, Natoli E, Rollins BJ, Milos PM. Monocyte chemoattractant protein-1 accelerates atherosclerosis in apolipoprotein E-deficient mice. *Arterioscler Thromb Vasc Biol*. 1999; 19:1518–1525.
21. Koyanagi M, Egashira K, Kitamoto S, Ni W, Shimokawa H, Takeya M, Yoshimura T, Takeshita A. Role of monocyte chemoattractant protein-1 in cardiovascular remodeling induced by chronic blockade of nitric oxide synthesis. *Circulation*. 2000;102:2243–2248.
22. Kitamoto S, Egashira K, Kataoka C, Koyanagi M, Katoh M, Shimokawa H, Morishita R, Kaneda Y, Sueishi K, Takeshita A. Increased activity of nuclear factor- κ B participates in cardiovascular remodeling induced by chronic inhibition of nitric oxide synthesis in rats. *Circulation*. 2000;102: 806–812.
23. Takemoto M, Egashira K, Usui M, Numaguchi K, Tomita H, Tsutsui H, Shimokawa H, Sueishi K, Takeshita A. Important role of tissue angiotensin-converting enzyme activity in the pathogenesis of coronary vascular and myocardial structural changes induced by long-term blockade of nitric oxide synthesis in rats. *J Clin Invest*. 1997;99:278–287.
24. Egashira K, Zhao Q, Kataoka C, Ohtani K, Usui M, Charo IF, Nishida K, Inoue S, Katoh M, Ichiki T, Takeshita A. Importance of monocyte chemoattractant protein-1 pathway in neointimal hyperplasia after periarterial injury in mice and monkeys. *Circ Res*. 2002;90:1167–1172.
25. Boring L, Gosling J, Cleary M, Charo IF. Decreased lesion formation in CCR2^{-/-} mice reveals a role for chemokines in the initiation of atherosclerosis. *Nature*. 1998;394:894–897.
26. Gu L, Okada Y, Clinton SK, Gerard C, Sukhova GK, Libby P, Rollins BJ. Absence of monocyte chemoattractant protein-1 reduces atherosclerosis in low density lipoprotein receptor-deficient mice. *Mol Cell*. 1998;2: 275–281.
27. Ni W, Egashira K, Kitamoto S, Kataoka C, Koyanagi M, Inoue S, Imaizumi K, Akiyama C, Nishida Ki K, Takeshita A. New anti-monocyte chemoattractant protein-1 gene therapy attenuates atherosclerosis in apolipoprotein E-knockout mice. *Circulation*. 2001;103:2096–2101.
28. Inoue S, Egashira K, Ni W, Kitamoto S, Usui M, Otani K, Ishibashi M, Hiasa K, Nishida K, Takeshita A. Anti-monocyte chemoattractant protein-1 gene therapy limits progression and destabilization of established atherosclerosis in apolipoprotein E-knockout mice. *Circulation*. 2002;106:2700–2706.
29. Ni W, Kitamoto S, Ishibashi M, Usui M, Inoue S, Hiasa K, Zhao Q, Nishida K, Takeshita A, Egashira K. Monocyte chemoattractant protein-1 is an essential inflammatory mediator in angiotensin II-induced progression of established atherosclerosis in hypercholesterolemic mice. *Arterioscler Thromb Vasc Biol*. 2004;24:534–539.
30. Roque M, Kim WJ, Gazdoin M, Malik A, Reis ED, Fallon JT, Badimon JJ, Charo IF, Taubman MB. CCR2 deficiency decreases intimal hyperplasia after arterial injury. *Arterioscler Thromb Vasc Biol*. 2002;22: 554–559.
31. Bush E, Maeda N, Kuziel WA, Dawson TC, Wilcox JN, DeLeon H, Taylor WR. CC chemokine receptor 2 is required for macrophage infiltration and vascular hypertrophy in angiotensin II-induced hypertension. *Hypertension*. 2000;36:360–363.
32. Sugaya T, Nishimatsu S, Tanimoto K, Takimoto E, Yamagishi T, Imamura K, Goto S, Imaizumi K, Hisada Y, Otsuka A, Uchida H, Sugiura M, Fukuta K, Fukamizu A, Murakami K. Angiotensin II type 1a receptor-deficient mice with hypotension and hyperreninemia. *J Biol Chem*. 1995; 270:18719–18722.
33. Sata M, Saiura A, Kunisato A, Tojo A, Okada S, Tokuhisa T, Hirai H, Makuuchi M, Hirata Y, Nagai R. Hematopoietic stem cells differentiate into vascular cells that participate in the pathogenesis of atherosclerosis. *Nat Med*. 2002;8:403–409.
34. Han KH, Tangirala RK, Green SR, Quehenberger O. Chemokine receptor CCR2 expression and monocyte chemoattractant protein-1-mediated chemotaxis in human monocytes: a regulatory role for plasma LDL. *Arterioscler Thromb Vasc Biol*. 1998;18:1983–1991.
35. Wang G, O K. Homocysteine stimulates the expression of monocyte chemoattractant protein-1 receptor (CCR2) in human monocytes: possible involvement of oxygen free radicals. *Biochem J*. 2001;357:233–240.
36. Liu Y, Liu T, McCarron RM, Spatz M, Feuerstein G, Hallenbeck JM, Siren AL. Evidence for activation of endothelium and monocytes in hypertensive rats. *Am J Physiol*. 1996;270:H2125–H2131.
37. Han KH, Han KO, Green SR, Quehenberger O. Expression of the monocyte chemoattractant protein-1 receptor CCR2 is increased in hypercholesterolemia: differential effects of plasma lipoproteins on monocyte function. *J Lipid Res*. 1999;40:1053–1063.
38. Ishibashi M, Egashira K, Hiasa K, Inoue S, Ni W, Zhao Q, Usui M, Kitamoto S, Ichiki T, Takeshita A. Antiinflammatory and antiarteriosclerotic effects of pioglitazone. *Hypertension*. 2002;40:687–693.

RESEARCH ARTICLE

Antimonocyte chemoattractant protein-1 gene therapy reduces experimental in-stent restenosis in hypercholesterolemic rabbits and monkeys

K Ohtani¹, M Usui¹, K Nakano¹, Y Kohjimoto², S Kitajima², Y Hirouchi², X-H Li³, S Kitamoto¹, A Takeshita¹ and K Egashira¹

¹Department of Cardiovascular Medicine, Graduate School of Medical Sciences, Kyushu University, Fukuoka, Japan; ²Primate Research Center, Guandong, China; and ³Gaoyao Kangda Laboratory Animals Science and Technology, Guandong, China

In-stent restenosis results exclusively from neointimal hyperplasia due to mechanical injury and a foreign body response to the prosthesis. Inflammation mediated by monocyte chemoattractant protein-1 (MCP-1) might therefore underlie in-stent restenosis. We recently devised a new strategy for anti-MCP-1 gene therapy by transfecting an N-terminal deletion mutant of the MCP-1 gene into skeletal muscles. We used this strategy to investigate the role of MCP-1 in experimental in-stent restenosis in hypercholesterolemic rabbits and monkeys. Transfection of the mutant

MCP-1 gene suppressed monocyte infiltration/activation in the stented arterial wall and markedly reduced the development of neointimal hyperplasia. This strategy also suppressed local expression of MCP-1 and inflammatory cytokines. Therefore, inhibition of MCP-1-mediated inflammation is effective in reducing experimental in-stent restenosis. This strategy might be a useful form of gene therapy against human in-stent restenosis.

Gene Therapy (2004) 11, 1273–1282. doi:10.1038/sj.gt.3302288; Published online 3 June 2004

Keywords: monocyte; inflammation; restenosis; stent

Introduction

Each year, more than 1.5 million patients undergo percutaneous coronary intervention of atherothrombotic lesions worldwide. Stent implantation is now the major revascularization technique.¹ Although the stent technique reduces the restenosis rate in selected coronary artery lesions, restenosis continues to occur in high-risk lesions or patients, and thus still remains an unsolved clinical issue. Anatomically, in-stent restenosis results exclusively from neointimal hyperplasia, whereas restenosis after balloon angioplasty results from neointimal hyperplasia and negative remodeling of the arterial wall.² There is a two-fold greater incidence of neointimal hyperplasia after stent implantation than after balloon angioplasty.³ Recent evidence suggests that in addition to mechanical injury, an intense foreign body response to stent prosthesis induces acute and chronic inflammation in the arterial wall, ensuing production of cytokines and growth factors that subsequently induce proliferation and migration of vascular smooth muscle cells.^{3,4,5} Experimental and clinical data suggest that inhibition of cellular proliferation with sirolimus might be an effective strategy to suppress in-stent restenosis.^{6–9}

There is growing evidence from clinical and animal studies indicating that inflammation is a central mediator

in restenosis.^{10–12} Recruitment and activation of monocytes/macrophages are major early histopathologic findings after arterial injury. As monocyte chemoattractant protein-1 (MCP-1) is a potent and specific chemokine for monocytes,^{13,14} an anti-inflammatory strategy targeting MCP-1 and its receptor (CCR2) might be an appropriate and reasonable approach for the treatment of restenosis. We recently devised a new strategy for anti-MCP-1 gene therapy by transfecting plasmid cDNA encoding a mutant MCP-1 gene into skeletal muscle.¹⁵ This mutant MCP-1 lacks N-terminal amino acids 2–8, called 7ND, forms inactive heterodimers with wild-type MCP-1, and thus works as a dominant-negative inhibitor of MCP-1.¹⁶ This method (intramuscular (i.m.) transfection of the gene) is useful because direct gene transfer into the injured arterial wall is not necessary and the role of MCP-1 can be investigated under pathophysiologic conditions *in vivo*. We used this strategy to demonstrate that blockade of the MCP-1 signal reduces neointimal hyperplasia after injury^{17,18,19} and atherosclerosis.^{20,21} Roque *et al*²² reported reduced neointimal hyperplasia after intraluminal arterial injury in CCR2-deficient mice. With regard to the role of MCP-1 in in-stent restenosis, Horvath *et al*²³ demonstrated that blockade of the MCP-1 receptor (CCR2) with anti-CCR2 antibody reduced neointimal hyperplasia by 40% after stenting by inhibiting monocyte infiltration in normocholesterolemic monkeys. In the latter study, however, the efficacy of CCR2 blockade might have been limited due to possible antigenic actions from the use of murine antibody in monkeys. Furthermore, because of the use of

Correspondence: Dr K Egashira, Department of Cardiovascular Medicine, Graduate School of Medical Science, Kyushu University, 3-1-1, Maidashi, Higashi-ku, Fukuoka 812-8582, Japan
Received 12 October 2003; accepted 19 March 2004; published online 3 June 2004

normocholesterolemic monkeys, the degree of stent-induced neointimal hyperplasia was markedly less than that reported in humans and in hypercholesterolemic animals.

Therefore, the primary aim of this study was to test the hypothesis that MCP-1-mediated arterial inflammation is the underlying mechanism in in-stent neointimal hyperplasia in hypercholesterolemic rabbits and monkeys, which might be more clinically relevant animal models than normocholesterolemic animals.²⁴

Results

Effects of 7ND gene transfer in rabbits

We measured gene expression of cytokines and chemokines 7 days after stenting (Figure 1a) (Table 1). The

mRNA levels of interleukin (IL)-6, tissue necrosis factor (TNF) α , IL-1 β , matrix metalloproteinases (MMP)-2, MMP-9, and vascular endothelial growth factor (VEGF) were higher in the stented artery than in the noninjured normal control artery. 7ND gene transfer did not affect the increase in mRNA levels of TNF α , MMP-2, and MMP-9, but reduced the increases in IL-6, IL-1 β , and VEGF levels. We immunohistochemically examined MCP-1 and VEGF expression and found that immunoreactive MCP-1 and VEGF increased 7 days after stenting (Figures 1b and c). Minor MCP-1 or VEGF immunostaining was detected in the noninjured control artery, whereas there was intense MCP-1 and VEGF immunoreactivity mainly in the media and intima 7 days after stenting. 7ND gene transfer markedly reduced the magnitude of MCP-1 and VEGF immunostaining (Figures 1b and c).

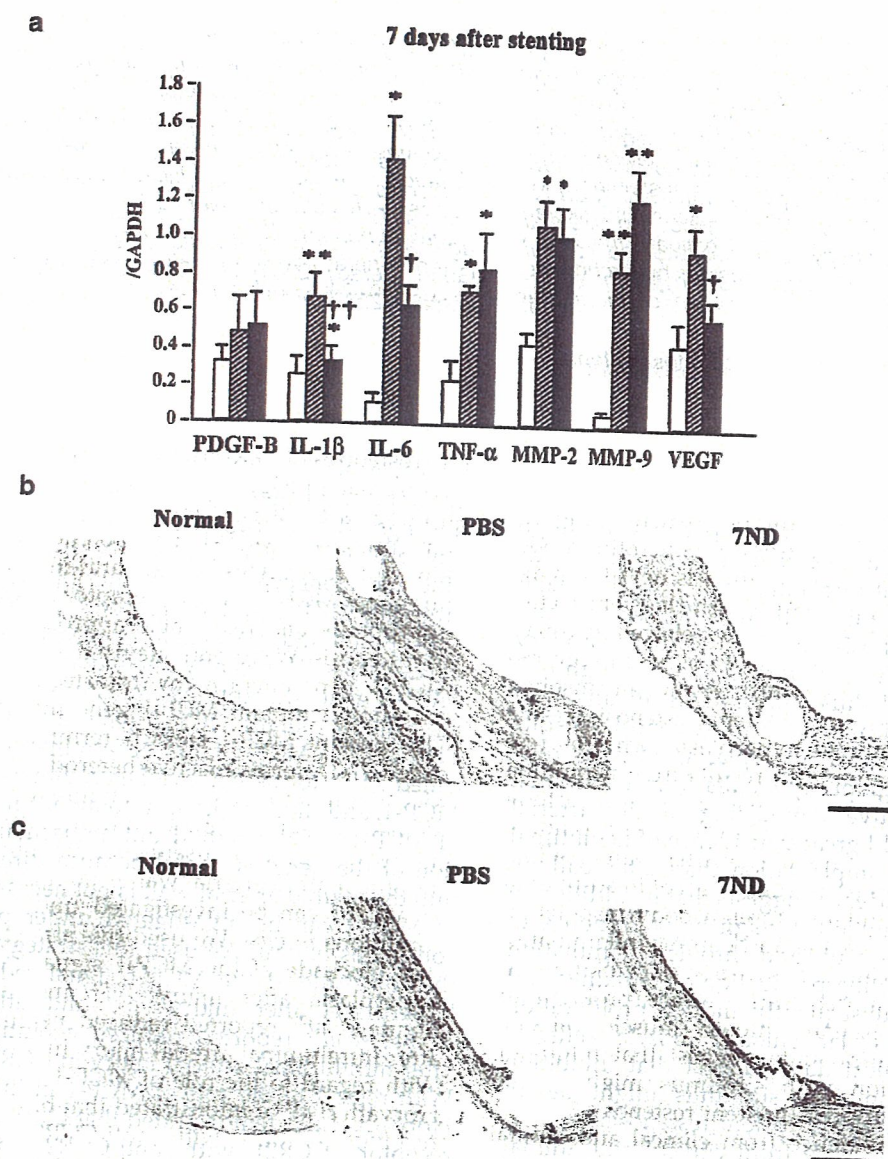


Figure 1 Gene expression and immunohistochemistry in the stented artery of rabbits. (a) Analysis of expression of various genes by real-time RT-PCR in noninjured controls (open bars) and stented arteries from PBS-treated rabbits (hatched bars) and stented arteries from rabbits transfected with 7ND gene (closed bars). $N=7-8$. * $P<0.05$, ** $P<0.01$ versus control (no injury); † $P<0.05$, †† $P<0.01$ versus the PBS group. (b) Arterial sections of control nonstented artery or stented arteries from the PBS-treated and 7ND-transfected group stained immunohistochemically with the antibody against MCP-1 7 days after stenting in rabbits. Bar = 200 μm . (c) Effects of 7ND gene transfer on protein expression of VEGF. Noninjured control artery section and stented artery sections from the PBS and 7ND group stained immunohistochemically with the antibody against VEGF. Bar = 200 μm .

Table 1 Probes used for real-time PCR

Assay	Sequence	Acc. no.
PDGF-B		
Forward	5'-CCCATCTACATCATCACCGAGTAC-3'	AB020215
Reverse	5'-GAGTGCTGCTGCAGGAAGGT-3'	
TaqMan probe	5'-TGGACTACCTGCACCGCAACAAGC-3'	
IL-6		
Forward	5'-CATGGTGCTGAAGAACATCCAA-3'	AF169176
Reverse	5'-ACTGGTTTTCTGCTGCAGGT-3'	
TaqMan probe	5'-AATGAAGAAGCCACCCTCAAGCCAGC-3'	
IL-1 β		
Forward	5'-TCAGCACCTCTCAGACAGAGTACAT-3'	M26295
Reverse	5'-AAGACACGAATTCATGCTGAA-3'	
TaqMan probe	5'-AAACAACAGTGGCGCCAAGACCTAA-3'	
TNF- α		
Forward	5'-CATGGTGCTGAAGAACATCCAA-3'	M12845
Reverse	5'-ACTGGTTTTCTGCTGCAGGT-3'	
TaqMan probe	5'-AATGAAGAAGCCACCCTCAAGCCAGC-3'	
MMP-2		
Forward	5'-GGAGAAGGCCGTGTTCTTTG-3'	D63579
Reverse	5'-CAGTGAAGCCCGCTCTAC-3'	
TaqMan probe	5'-CCAAGCCTTGACCAGCCTCGG-3'	
MMP-9		
Forward	5'-GCAGGATGTCAAAGCTCACGTA-3'	D26514
Reverse	5'-AACACACACGACGCTTCCAGTA-3'	
TaqMan probe	5'-TCACACGCCAGAAGAAGCGGTCC-3'	
VEGF		
Forward	5'-GGCTGCTGCAATGATGAAAG-3'	AB020216
Reverse	5'-TTGATCCGCATGATCTGCAT-3'	
TaqMan probe	5'-TGCCACCGAGGAGTTCAACGTC-3'	
GAPDH		
Forward	5'-CTCTGGCAAAGTGGATGTTGTC-3'	L23961
Reverse	5'-GGGTGGAATCATACTGGAACATG-3'	
TaqMan probe	5'-CCATCAATGATCCATTGACCTCCA-3'	

Acc. no. indicates the accession number in GenBank.

Vascular inflammation, proliferation, and apoptotic cell death were examined 7 days after stent implantation. Infiltration of monocytes/macrophages (Figure 2a) and appearance of proliferating cells (Figure 2b) were observed in the intima and media. Apoptotic cells (Figure 2c) were observed in the intima. Increased inflammation, proliferation, and apoptotic cell death persisted mainly in the neointima at 28 days (data not shown). 7ND gene transfer attenuated the inflammation and proliferation, and enhanced cell death after stenting (Figure 2). There were equal numbers of endothelial cells, monitored by CD31 immunoreactivity in animals treated with phosphate-buffered saline (PBS) or transfected with 7ND gene (Figure 2d). Neointimal hyperplasia was examined by intravascular ultrasound (IVUS) and by histopathologic analysis 28 days after stenting (Figure 3). We detected significant neointimal hyperplasia 28 days after stenting in the PBS-treated rabbits. 7ND gene transfer markedly reduced the neointimal formation as assessed by ultrasonographic and histologic analyses (Figure 3).

We measured plasma and femoral muscle concentrations of 7ND after 7ND or empty plasmid transfection.

Plasma 7ND was detected in the plasma 3, 7, and 14 days after 7ND transfection (Table 2). On day 3 of transfection, 7ND could be detected only in 7ND-transfected muscle (Table 3). These data confirm that 7ND protein was released from transfected muscles to circulation.

Effects of 7ND gene transfer in monkeys

Histopathologic and immunohistochemical analyses were performed 28 days after stenting (Figure 4). MCP-1 immunoreactivity was not detected in the nonstented artery (data not shown), whereas intense MCP-1 and CCR2 immunoreactivity was evident mainly in the neointima around the stent prosthesis and weakly in the media (Figure 4a). As seen in rabbits, 7ND gene transfer reduced the magnitude of MCP-1 immunostaining (data not shown) and the neointimal formation (Figures 4b and c).

Effects of 7ND gene transfer in cholesterol levels

In rabbits, the total cholesterol levels before and 28 days after stenting were 922 ± 108 and 968 ± 166 mg/dl in the PBS-treated group, and 938 ± 74 and 950 ± 117 mg/dl in 7ND-transfected group. In monkeys, the total cholesterol

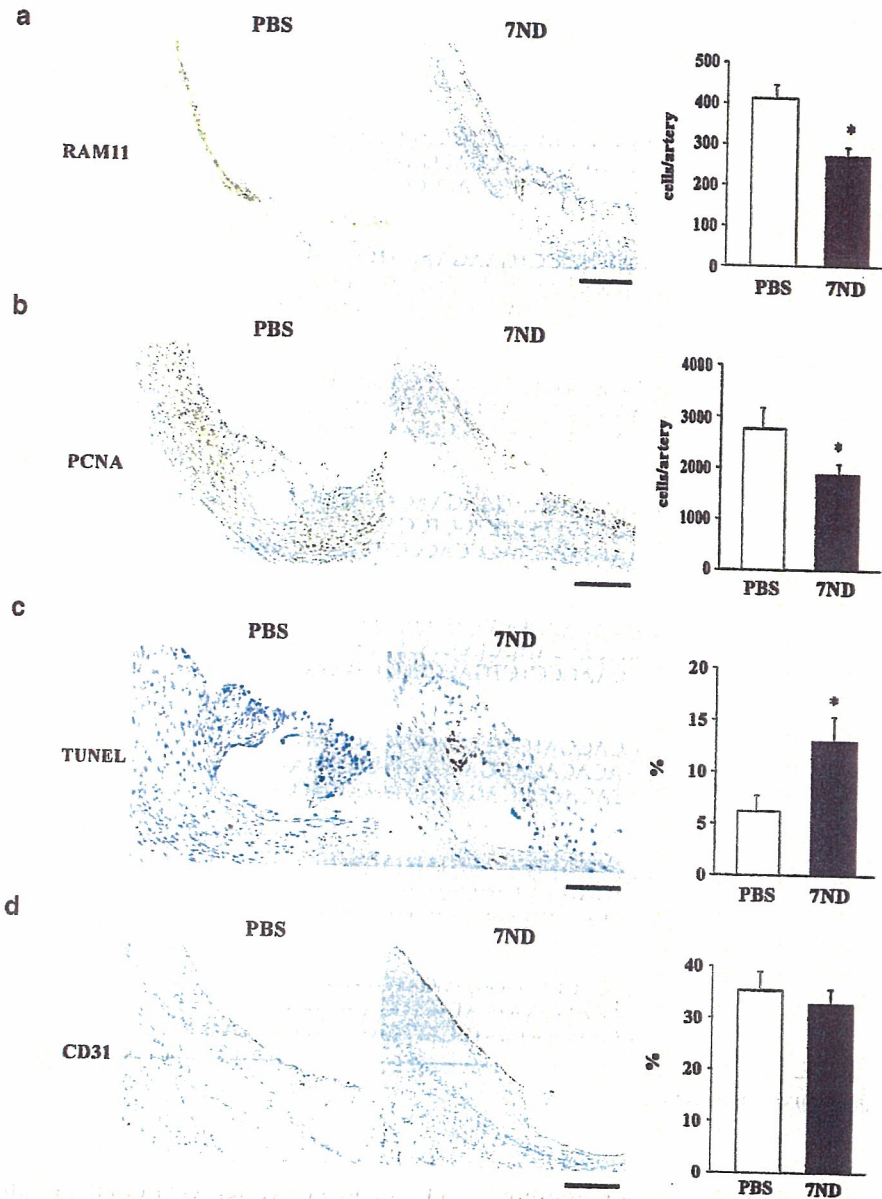


Figure 2 Inflammation, proliferation, and cell death in the stented artery of rabbits. (a) Effects of 7ND gene transfer on inflammatory changes. Artery sections 7 days after stenting from a rabbit transfected with PBS and a rabbit transfected with 7ND plasmid immunohistochemically stained for monocytes/macrophages (RAM11) and summary of quantitative analyses are presented ($n = 8$ each). $*P < 0.01$ versus PBS. Bar = 200 μm . (b) Effects of 7ND gene transfer on proliferative changes. Artery sections 7 days after stenting immunohistochemically stained for PCNA and summary of quantitative analyses are presented ($n = 8$ each). $*P < 0.01$ versus PBS. Bar = 200 μm . (c) Effects of 7ND gene transfer on cell death. TUNEL-stained artery sections 7 days after stenting and summary of quantitative analyses are presented ($n = 8$ each). $*P < 0.05$ versus PBS. Bar, 100 μm . (d) Effects of 7ND gene transfer on CD31-positive endothelial lining 7 days after stenting and summary of quantitative analyses are presented ($n = 8$ each). Bar, 100 μm .

levels before and 28 days after stenting were 444 ± 43 and 429 ± 37 mg/dl in the PBS-treated group, and 469 ± 30 and 488 ± 44 mg/dl in 7ND-transfected group. These data indicate that the observed effects of 7ND gene transfer were not due to changes in serum cholesterol levels.

Antibody production in 7ND-transfected monkeys

In ELISA assay, IgG and IgM antibodies against 7ND protein were not detected after 7ND transfection ($n = 6$ each, Figure 5).

Discussion

The present study demonstrated that blockade of MCP-1 by 7ND gene transfer attenuated monocyte infiltration, and thus suppressed the development of neointimal formation after stent placement in hypercholesterolemic rabbits and non-human primates (cynomolgus monkeys), indicating a role of MCP-1 in stent-induced experimental restenosis (neointimal formation).

Recent studies suggested that inflammation is an important determinant of in-stent neointimal hyperplasia. Inflammation associated with coronary stenting was

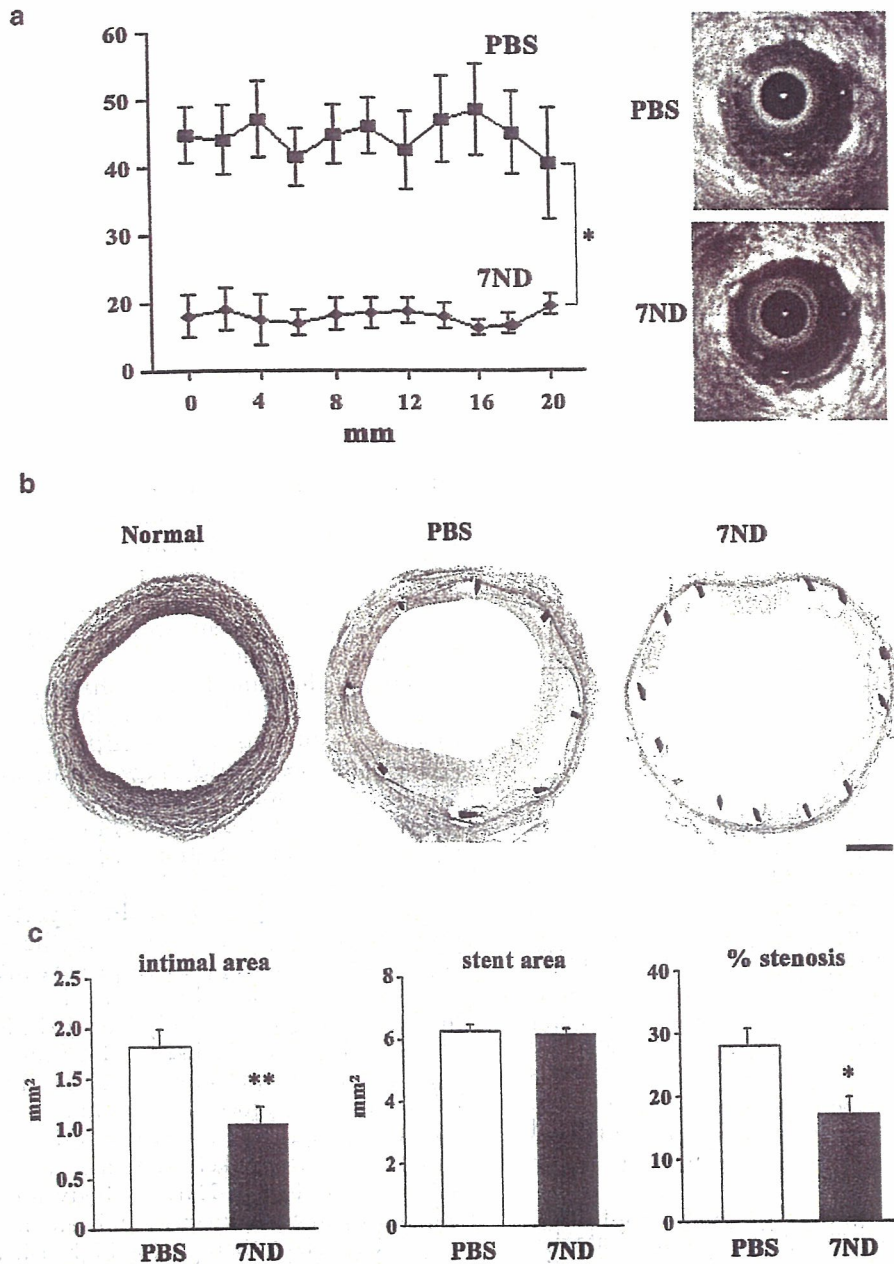


Figure 3 Effects of 7ND gene transfer on in-stent neointimal hyperplasia in rabbits. (a) Left: mean percent area stenosis within stent in the PBS-treated and 7ND-transfected rabbits as assessed by intravascular ultrasound. X-axis: distance from the distal to the proximal stent end; Y-axis: % cross-sectional stenosis. The upper right panel shows an intravascular ultrasound cross-section image in PBS-treated animal with large neointimal hyperplasia. The lower right panel displays an intravascular ultrasound cross-section image in 7ND-transfected animal with small neointimal hyperplasia. * $P < 0.01$ between PBS and 7ND. (b) Noninjured control artery section (left panel) and artery sections from the PBS-treated group (middle panel) and 7ND-transfected group (right panel) 28 days after stenting stained with elastic van-Gieson in rabbits. Bar = 600 μm . (c) Effect of 7ND gene transfer on intimal area, stented area, and % stenosis 28 days after stenting in rabbits ($n = 8$ each). * $P < 0.05$, ** $P < 0.01$ versus PBS.

described previously^{3,10}; neutrophils surrounding stent struts are observed only transiently within early stages, whereas chronic inflammatory cells such as monocytes are observed both in early (within 7 days) and late stages (6 months or later) after stenting. Increased monocyte inflammation is associated with greater neointimal formation after stenting in animals²⁵ and humans.¹⁰ Furthermore, a monoclonal antibody against the adhesion molecule Mac-1 reduced monocyte recruitment and neointimal formation after rabbit iliac artery stenting.²⁶ As inflammation is unavoidable during stent placement, therapies directed against stent-induced inflammation

are a reasonable approach to reduce stent-associated restenosis. Recent experimental studies indicate that a drastic reduction in neointimal formation with rapamycin-eluting stents is mediated by its antiproliferative and anti-inflammatory effects.⁶

There is a rapid increase in plasma MCP-1 within the first day of coronary intervention.^{27,28} Persistent increase in MCP-1 after angioplasty is a significant and independent predictor of restenosis.²⁷ We demonstrated increased immunostaining of MCP-1 after stenting. 7ND gene transfer markedly attenuated inflammatory and proliferative changes and increased apoptotic cell death,

Table 2 Plasma concentrations of 7ND after empty or 7ND plasmid transfection in rabbits

	Baseline	Days after transfection			
		3	7	14	28
No transfection (pg/ml)	<20.0 (below detectable limits)	<20.0	<20.0	<20.0	<20.0
Empty plasmid transfection (pg/ml)	<20.0	<20.0	<20.0	<20.0	<20.0
7ND transfection (pg/ml)	<20.0	96 ± 19	76 ± 15	63 ± 9	<20.0

Values are mean ± s.e.m., $n = 6-8$.

Table 3 Tissue concentrations of 7ND 3 days after empty or 7ND plasmid transfection in rabbits

	Tissue (pg/mg)
No transfection	<20.0
Empty plasmid transfection	<20.0
7ND plasmid transfection	306 ± 39

Values are mean ± s.e.m., $n = 5-6$.

and thus suppressed in-stent neointimal hyperplasia. Our present data, therefore, suggest that locally produced MCP-1 not only induced the recruitment of monocytes but also activated lesional monocytes and vascular smooth muscle cells to produce the inflammatory cytokines and growth factors (IL-6, IL-1 β , VEGF), which in turn might result in in-stent neointimal hyperplasia. We previously reported that 7ND gene transfer suppressed neointimal formation after balloon or cuff injury.¹⁷⁻¹⁹ The present study therefore extends our previous reports with regard to the beneficial effects of 7ND gene transfer on balloon or cuff injury-induced neointimal hyperplasia to in-stent neointimal hyperplasia.

Our finding in non-human primates might have clinical significance, because many therapeutic strategies that have proven effective in reducing restenosis in nonprimate animal model failed to demonstrate a substantial effect on human restenosis. Horvath *et al*²³ demonstrated that injection of an antibody against murine CCR2 attenuated neointimal hyperplasia after iliac arterial stenting in normocholesterolemic cynomolgus monkeys. The magnitude of inflammation and neointimal formation, however, was markedly less in the study by Horvath *et al*²³ (mean intimal thickness in animals with no treatment: 0.25 ± 0.03 mm) than in the present study (0.33 ± 0.02 mm) and those reported in humans^{3,10} (0.3-0.5 mm). Small-scale neointimal formation is also reported in normocholesterolemic rabbits (0.13 ± 0.03 mm).²⁹ This difference might be because hypercholesterolemic animals were used in the present study. Although the appropriate animal model for evaluation of experimental in-stent restenosis is uncertain, the hypercholesterolemic non-human primate model might have an advantage over normocholesterolemic nonprimate animal models, because (1) adequate

degrees of neointimal hyperplasia develop after stenting and (2) vascular inflammatory and proliferative responses to injury in non-human primates are presumed to be closer to those in humans than other nonprimate models. Therefore, the use of non-human primates might allow us to evaluate the efficacy of therapies such as 7ND gene transfer on in-stent neointimal hyperplasia under more reliable conditions.

Although this anti-MCP-1 therapy by 7ND gene transfer has yet to be tested for the prevention of restenosis in humans, the beneficial effects observed in rabbit and monkey models suggest a significant potential for this new mode of treatment. For translational research, we must determine as to what is the effective range of 7ND concentration in humans. Basal plasma levels of MCP-1 protein in patients before PCI are reported to be 500 pg/ml.²⁷ Other reports show plasma MCP-1 levels in patients to be in the range of 150-852 pg/ml.^{28,30,31} Compared to plasma MCP-1 levels in humans, 7ND levels achieved by i.m. transfection of 7ND gene in the present study seem to be less. Therefore, further studies are needed to determine the effective range of 7ND concentration in humans before this anti-MCP-1 strategy proceeds to clinical study. As no antibody against 7ND protein was detected after 7ND transfection, it is unlikely that the observed effects of 7ND were due to anti-7ND antibody formation. If this mode of treatment is effective and safe, it could be used as an independent therapy for high-risk lesions, small vessels (<2.5 mm in diameter), or recurrent restenosis. It could also be used as an adjunct therapy for restenosis after drug-eluting stents. 7ND-eluting stents might be associated with a drastic reduction in restenosis in humans.

In conclusion, this study provides evidence that MCP-1-mediated inflammation is an essential mediator in the development of experimental restenosis (neointimal formation) after stenting. Inhibition of stent-associated inflammation by 7ND gene transfer might be a promising next-generation gene therapy to reduce restenosis and to improve clinical outcome after stent placement.

Materials and methods

Plasmid expression vectors

Human 7ND cDNA was constructed by recombinant polymerase chain reaction (PCR) using a wild-type human MCP-1 cDNA (Dr T Yoshimura, National Cancer

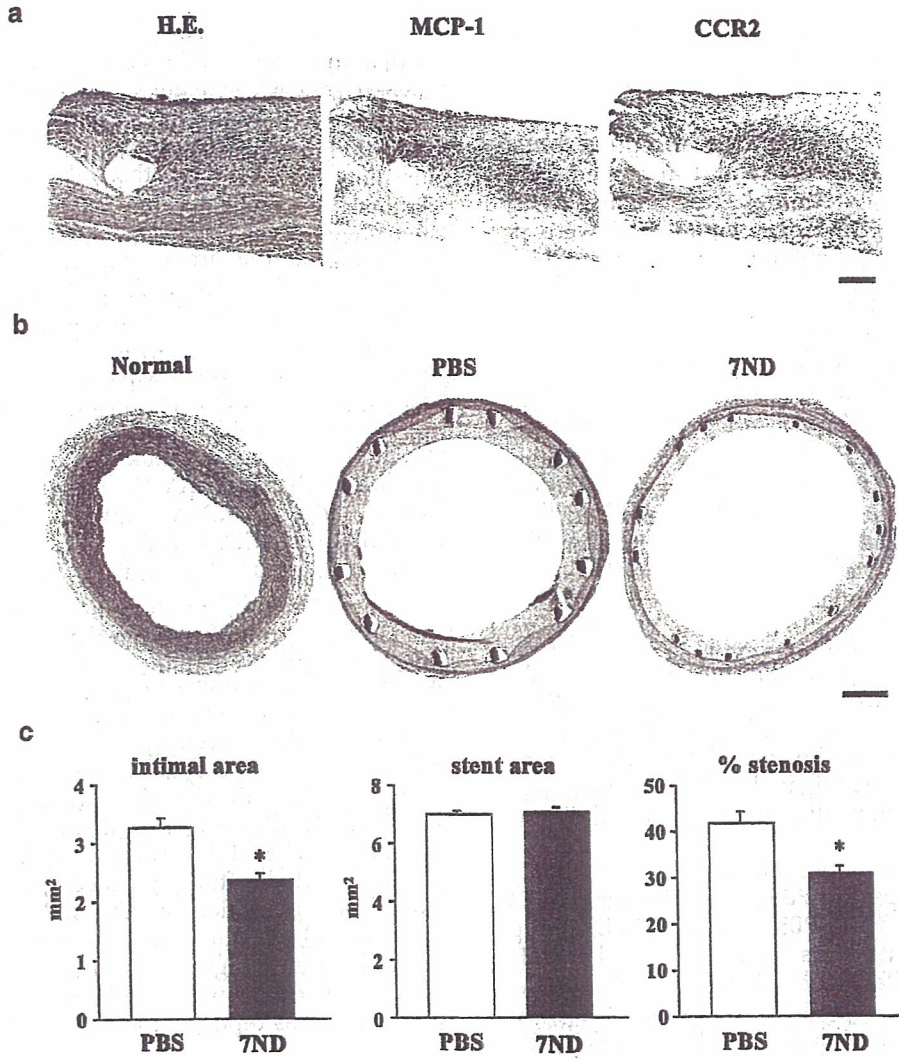


Figure 4 Effects of 7ND gene transfer on in-stent neointimal hyperplasia in cynomolgus monkeys. (a) Arterial sections of stented artery from the PBS group stained with HE or immunohistochemically with the antibodies against MCP-1 and CCR2 28 days after stenting in monkeys. Bar = 100 μ m. (b) Noninjured control artery section (left panel) and artery sections from the PBS-treated group (middle panel) and 7ND-transfected group (right panel) 28 days after stenting stained with elastic van-Gieson in monkeys. Bar = 500 μ m. (c) Effect of 7ND gene transfer on stented area, intimal area, and % stenosis 28 days after stenting (n = 8 each). *P < 0.01 versus PBS.

ELISA assay of anti-7ND antibody

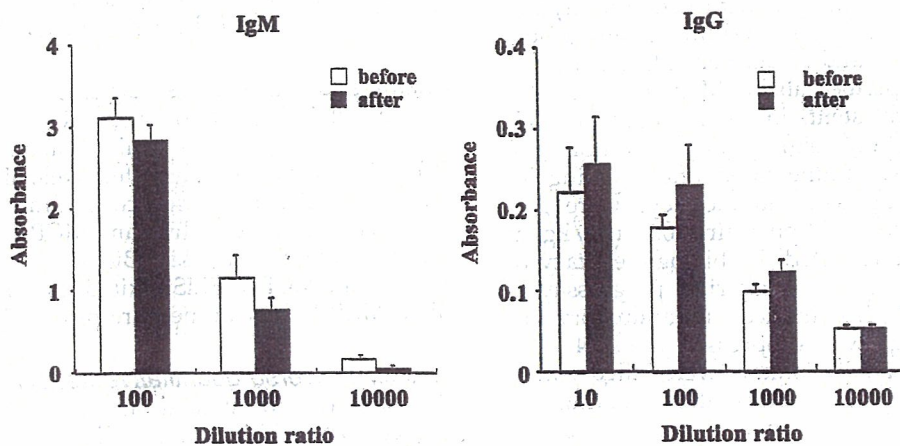


Figure 5 ELISA assay of anti-7ND antibody (IgM and IgG) in paired serum from 7ND-transfected monkeys.

Institute, Japan) as a template and inserted into the BamHI (5') and NotI (3') sites of the pcDNA3 (Invitrogen) expression vector plasmid.¹⁵

Animal model of in-stent restenosis and gene transfer

The experiments were reviewed and approved by the Committee on Ethics on Animal Experiments, Kyushu University Faculty of Medicine, Japan, and were performed according to the Guidelines of American Physiologic Society. A part of this study was performed at the Kyushu University Station for Collaborative Research and the Morphology Core, Japan.

Male Japanese white rabbits (KBT Oriental, Tokyo, Japan) weighing 3.0–3.5 kg were fed a high cholesterol diet containing 1% cholesterol and 3% peanut oil for 2 weeks. They were then anesthetized by i.m. injection of xylazine (5 mg/kg) and ketamine (35 mg/kg). The right common carotid arteries were surgically exposed, and a 3F Fogarty balloon catheter was passed into one iliac artery under fluoroscopic guidance, and the balloon was then withdrawn and inflated over a 3-cm section of artery three times; then, a 15 mm-long Multilink stent (RX Multi-link plus, Guidant/ACS Inc.) mounted over the 3-mm balloon was implanted in the iliac artery (30-s inflation, 10 atm, stent-to-artery ratio of 1.2:1.0). When the stent was intended to be implanted bilaterally, the procedure was repeated in the contralateral iliac artery. The carotid artery was then ligated and the incision was closed. After the operation, all rabbits were fed the same high cholesterol diet.

At 3 days before stenting, rabbits were randomly divided into two groups: the PBS group (16 stents in 14 rabbits) was injected with PBS and the 7ND group (16 stents in 14 rabbits) was injected with the 7ND gene (500 µg/0.3 ml PBS) into their femoral muscle. To enhance transgene expression, all plasmid-injected animals received electroporation at the injection site immediately after injection with an electric pulse generator CUY21 (BTX, San Diego, CA, USA) as described previously.^{17,19} All rabbits were killed with a lethal dose of anesthesia 7 or 28 days after stenting for biochemical, immunohistochemical, and morphometric analyses. IVUS study was also performed 28 days after stenting.

Male adult cynomolgus monkeys (5 years old) weighing 4–5 kg were purchased from Primate Ltd., Kumamoto, Japan and were fed laboratory diet containing 0.5% cholesterol starting 2 months before stent implantation. Monkeys were anesthetized with ketamine hydrochloride (10 mg/kg i.m.) and sodium pentobarbital (30 mg/kg i.v. to effect), and underwent placement of a 3 × 15 mm² stent as described above. Monkeys were also injected with PBS (eight stents in six monkeys) or 7ND plasmid (2.5 mg/500 µl PBS, eight stents in six monkeys) into their femoral muscle immediately after stenting. To enhance transgene expression, all monkeys were pre-treated with i.m. injection of bupivacaine (0.25 mg/kg) at the injection site.¹⁷ We reported the biologic efficacy of 7ND gene transfer using *in vivo* matrigel plug assay in monkeys.¹⁷ In brief, MCP-1-induced inflammatory angiogenesis in the plugs was suppressed until 14 days after 7ND gene transfer. All monkeys were killed with a lethal dose of anesthesia 28 days after stenting for morphometric analysis. All animals received aspirin 81 mg/day and ticlopidine 100 mg/day until euthanasia.

Histopathology and immunohistochemistry

Stented arterial segments were excised and fixed for 24 h with 6–10% paraformaldehyde or methacarn solution for several days. Each segment was divided into two parts at the center of the stent. The proximal part was embedded in methyl methacrylate mixed with *n*-butyl methacrylate to allow for sectioning through metal stent struts. Sections were stained with elastica van Gieson and hematoxylin–eosin (HE). To evaluate the thickening of the neointima, the areas encroached by the external elastic lamina, the internal elastic lamina, and the lumen area were measured. The distal part was used for immunohistochemical analysis. After stent struts were gently removed with microforceps, the tissue was dehydrated, embedded in paraffin, and cut into 5-µm thick slices. In rabbits, the sections were subjected to immunostaining using antibodies against rabbit monocytes/macrophages (RAM11, Dako), proliferating cell nuclear antigen (PCNA) (Dako), MCP-1 (R & D), endothelial cell (CD31, Dako), VEGF (Santa Cruz), or non-immune mouse IgG (Dako). The cells that underwent apoptosis were detected by using terminal deoxynucleotidyl transferase-mediated dUTP nick end-labeling (TUNEL) staining (*in situ* apoptosis detection kit, Takara). The number of apoptotic nuclei in arterial wall was counted, and the data were calculated and expressed as the percentage of apoptotic cells nuclei/total nuclei. In monkeys, the sections were immunohistochemically stained with antibodies against MCP-1 (R & D), CCR2 (Sigma Chemical), or non-immune mouse IgG (Dako). The slides were washed and incubated with biotinylated, affinity-purified goat IgG. Following avidin-biotin amplification, the slides were incubated with diaminobenzidine and counterstained with hematoxylin. The percentage of immunopositive cells per total cells in each section was calculated, and the average of five sections was reported for each animal.

Intravascular ultrasound procedure and analysis

High-resolution IVUS analysis was performed 28 days after stenting with an electron-scan IVUS system (Terumo TU-C100, Tokyo, Japan). A contour detection program was used for two-dimensional analysis. Quantitative IVUS measurements were performed at 10 cross-sections in each stent segment at 2-mm intervals from the distal stent end. Cross-sectional narrowing was calculated as the neointimal area divided by stent area. All the measurements were performed by a single sonographer who was unaware of the experimental protocol.

Plasma and tissue measurements

Plasma total cholesterol and LDL cholesterol were measured using a commercially available kit. To measure 7ND released by the transfected skeletal muscle, plasma and femoral skeletal muscle concentrations of 7ND were measured using the human MCP-1 enzyme-linked immunosorbent assay kit (Biosource) in rabbits.¹⁹ As this human MCP-1 ELISA kit does not react with the rabbit MCP-1, we can measure plasma 7ND in rabbits.

Real-time reverse quantitative transcription-PCR

The normal and stented arteries were excised and washed with cold normal saline 7 days after stent placement. Stent was removed gently. The samples were